Supporting Information for:

CO_2 Reduction with Protons and Electrons at a Boron-Based Reaction Center

Jordan W. Taylor, Alex McSkimming, Laura A. Essex and W. Hill Harman*

Department of Chemistry, University of California-Riverside, Riverside, CA 92501
Email: hill.harman@ucr.edu

Contents

Synthetic Procedures

General considerations. Unless otherwise noted, all manipulations were carried out using standard Schlenk or glovebox techniques under a N_2 atmosphere. Hexanes, benzene, toluene, and acetonitrile were dried and deoxygenated by argon sparge followed by passage through activated alumina in a solvent purification system from JC Meyer Solvent Systems followed by storage over 4 Å molecular sieves. THF and Et_2O were distilled from sodium-benzophenone ketyl under N_2 followed by storage over 4 Å molecular sieves for at least 24 hours prior to use. Non-halogenated and non-nitrile containing solvents were tested with a standard purple solution of sodium benzophenone ketyl in THF to confirm effective oxygen and moisture removal prior to use. Hexamethyldisiloxane (HMDSO) was distilled from sodium metal and stored over 4 Å molecular sieves for 24 hours prior to use. All reagents were purchased from commercial suppliers and used without further purification unless otherwise noted. $Au(B_2P_2)Cl$ (**3**), $Au(B_2P_2)$ (**4**), $[Au(B_2P_2)][K(18\text{-c-}6)]$ (**1**),[1] DBU•HCl,[2] and $Na(C_{10}H_8)$ were synthesized according to literature procedures.[3] Elemental analyses were performed by Midwest Microlab, LLC, Indianapolis, IN. Deuterated solvents were purchased from Cambridge Isotope Laboratories Inc., degassed, and dried over activated 3 Å molecular sieves for at least 24 h prior to use. NMR spectra were recorded on Varian Inova 500 MHz, Bruker Avance 600 MHz, and Bruker Avance 700 MHz spectrometers. ^1H and ^{13}C chemical shifts are reported in ppm relative to tetramethylsilane using residual solvent as an internal standard. Original ^{11}B NMR spectra were processed using MestReNova 10.0.2 with a backwards-linear prediction applied to eliminate background signal from the borosilicate NMR tube.[4] For ^{11}B NMR spectra with peaks overlapping the borosilicate signal, a manual baseline correction was applied. IR spectra were recorded using a Bruker Alpha FTIR with a universal sampling module collecting at 4 cm^{-1} resolution with 32 scans. X-ray diffraction studies were performed using a Bruker-AXS diffractometer. Cyclic Voltammetry (CV) experiments were performed using a Pine AFP1 potentiostat. The cell consisted of a glassy carbon working electrode, a Pt wire auxiliary electrode and a Pt wire pseudo-reference electrode. All potentials are referenced vs. the Fc/Fc^+ couple measured as an internal standard.

$Au(B_2P_2)H$ (2). *from K[sec-Bu_3BH]*: **3** (0.050 g, 0.063 mmol) was suspended in Et_2O (4 mL) before adding K[*sec*-Bu_3BH] (63 μL, 0.063 mmol, 1.0 M in THF) as an Et_2O solution (2 mL). The reaction was stirred 30 minutes during which time a colorless precipitate developed in a pale-yellow solution. The reaction was filtered through celite, concentrated *in vacuo* (ca. 2 mL), and hexanes (4 mL) added before further concentration *in vacuo* caused the product to precipitate. The product was rinsed with hexanes (2 x 1 mL) and dried *in vacuo*. Yield: 0.030 g, 64%.

from $HSiEt_3$: **3** (0.050 g, 0.063 mmol) was suspended in toluene (4 mL) before adding $HSiEt_3$ (0.029 g, 0.252 mmol) as a toluene solution (2 mL). The reaction was stirred 1 hour where it became homogenous. The reaction was concentrated *in vacuo* (ca. 2 mL) and HMDSO (4 mL) added before further concentration *in vacuo* caused the product to precipitate. The product was rinsed with hexanes (2 x 1 mL) and dried *in vacuo*. Additional crops could be obtained by further concentration and HMDSO (ca.1 mL) addition to the mother liquor. Yield: 0.040 g, 84%.

from H_2/DBU: **3** (0.010 g, 0.019 mmol) was dissolved in THF (0.6 mL), DBU (2.84 μL, 0.019 mmol) added, and the resulting mixture subjected to three freeze-pump-thaw cycles before the adding of 1 atm of H_2. The reaction mixture was sonicated for 10 minutes and the volatiles removed *in vacuo.* The resulting pale-yellow foam was dissolved in toluene (2 x 1 mL) and filtered through celite. Removal of volatiles from the filtrate *in vacuo* furnished the product as a pale yellow solid. Yield: 0.009 g, 95%.

from $HSnBu_3$: **4** (0.050 g, 0.063 mmol) was dissolved in THF (2 mL) and $HSnBu_3$ (0.020 g, 0.069 mmol) added as a THF (1 mL) solution. The reaction was stirred 12 hours during which time a pale-yellow solution formed. The reaction was concentrated *in vacuo* (ca. 1 mL) before adding HMDSO (2 mL). Further concentration *in vacuo* induced crystallization of the product as a yellow solid that was collected, rinsed with hexanes (2 x 1 mL), and dried *in vacuo*. Yield: 0.042 g, 89%.

from DBU•HCl: **1** (0.015 g, 0.014 mmol) was dissolved in MeCN (2 mL) and DBU•HCl (0.002 g, 0.014 mmol) was added as a MeCN (1 mL) solutionThe reaction immediately became pale yellow and the volatiles were removed *in vacuo*. The pale-yellow residue was rinsed with hexanes (2 x 1 mL), dissolved in toluene (2 mL), and filtered through celite. Volatiles were removed from the filtrate *in vacuo* to yield the product as a pale yellow solid. Pre- and post-reaction ^{1}H, ^{31}P, ^{11}B NMR spectra are shown in Figures S5–7. Yield: 0.011 g, 98%. X-ray quality crystals were grown by layering a concentrated toluene solution with HMDSO. ^{1}H NMR (500 MHz, C_6D_6) δ 8.95 (bs, 1H), 7.86 (d, J = 6.9 Hz, 2H), 7.61 (m, 1H), 7.50 (d, J = 7.4 Hz, 1H), 7.44 (d, J = 7.5 Hz, 2H), 7.31 (m, 2H), 7.27 (t, J = 7.3 Hz, 1H), 7.18 (m, 2H), 7.12 (t, J = 7.3 Hz, 1H), 7.03 (t, J = 7.2 Hz, 2H), 5.09 (m, J_{BH} = 80 Hz, 1H), 1.97 (m, 4H), 0.76 (d, J = 6.9 Hz, 6H), 0.73 (d, J = 7.1 Hz, 6H), 0.71 (d, J = 7.1 Hz, 3H), 0.68 (d, J = 6.9 Hz, 3H), 0.55 (d, J = 7.0 Hz, 3H), 0.52 (d, J = 6.9 Hz, 3H). ^{31}P{^{1}H} NMR (202 MHz, C_6D_6) δ 58.39 (d, J = 255.3 Hz), 55.91 (d, J = 255.0 Hz). ^{11}B NMR (193 MHz, THF:Benzene, 3:1) δ 52.45, −10.01 (d, J = 78.4 Hz). ^{13}C NMR (126 MHz, C_6D_6) δ 145.6 (d, J = 14.2 Hz), 142.1, 138.0, 135.7, 134.5 (d, J = 11.0 Hz), 134.2 (d, J = 10.5 Hz), 131.4 (d, J = 15.2 Hz), 130.7 (d, J = 13.7 Hz), 129.9, 126.3 (d, J = 6.0 Hz), 124.9 (d, J = 6.6 Hz), 122.7, 28.7 (d, J = 26.1 Hz), 27.4 (d, J = 25.7 Hz), 20.6 (d, J = 4.9 Hz), 20.1 (m), 19.7 (d, J = 3.7 Hz), 19.4. FTIR: ν_{max} (cm^{-1}) 2838, 2119 (B-H). Anal. Calcd for $C_{36}H_{45}AuB_2P_2$: C, 57.02 H, 5.98. Found: C, 56.89 H, 5.96.

Au(B_2P_2)(O_2CH) (5). A solution of **1** (0.020 g, 0.026 mmol) in benzene (3 mL) was subjected to three freeze-pump-thaw cycles prior to adding 1 atm CO_2. The reaction was stirred 30 minutes, and the volatiles were removed *in vacuo* to yield the product as a pale-yellow solid. Yield: 0.019 g, 90%. X-ray quality crystals were grown by layering a concentrated THF solution with hexanes. A sample suitable for element analysis was prepared by layering a concentrated $CDCl_3$ solution with hexanes. ^{1}H NMR (500 MHz, $CDCl_3$) δ 8.40 (bs, 1H), 8.30 (d, J = 7.1 Hz, 2H), 7.69 (s, 1H), 7.64 (t, J = 7.3 Hz, 2H), 7.54-7.49 (m, 2H), 7.42 (t, J = 7.5 Hz, 2H), 7.18 (dd, J = 5.3, 3.4 Hz, 4H), 7.07 (dd, J = 5.5, 3.3 Hz, 2H), 7.03 (bs, 2H), 2.46-2.36 (m, 4H), 0.98 (d, J = 8.5 Hz, 6H), 0.95 (d, J = 8.3 Hz, 6H), 0.84 (d, J = 7.8 Hz, 6H), 0.81 (d, J = 7.8 Hz, 6H). ^{31}P{^{1}H} NMR (202 MHz, $CDCl_3$) δ 56.1 (s). ^{11}B{^{1}H} (193 MHz, $CDCl_3$) δ 26.9 (bs). ^{13}C NMR (126 MHz, $CDCl_3$) δ 168.2, 160.6, 153.1, 136.5, 136.1, 133.5 (t, J = 8.0 Hz), 131.6, 131.4, 131.3 (t, J = 26.4 Hz), 130.6, 130.2, 129.20, 128.5, 128.4, 126.0, 125.4, 28.4 (t, J = 14.2 Hz), 20.2, 19.7. FTIR: ν_{max} (cm^{-1}) 1672 (C=O). Anal. Calcd for $C_{37}H_{45}AuB_2O_2P_2$ (1 x $CDCl_3$): C, 49.52 H, 5.03. Found: C, 49.49 H, 5.51.

*Reaction of **5** with Na($C_{10}H_8$).* **5** (0.015 g, 0.019 mmol) was dissolved in THF (1 mL), and a solution of Na($C_{10}H_8$) (0.004 g, 0.019 mmol) in THF (1 mL) was added at room temperature. A color change to purple occurred immediately concomitant with the formation of a small amount of precipitate. The reaction was filtered through a celite-packed pipette, and the filter was removed from the glovebox. The filter was dried with a stream of air and rinsed with D_2O into an NMR tube. ^{1}H NMR revealed a resonance at δ 8.28 ppm that was in agreement with the reported literature value for sodium formate.[5] See Figure S12 for the collected spectra.

Reaction of **5** *with HCl•Et_2O.* **5** (0.012 g, 0.015 mmol) was dissolved in $CDCl_3$ (1 ml), and HCl•Et_2O (10 μl, 0.020 mmol, 2.0 M in Et_2O) was added at room temperature. The reaction was stirred 30 minutes before collecting ^1H and ^{31}P NMR data that matched the reported spectra.[19] The sample used for NMR spectroscopy was then crystallized by layering with hexanes (1 mL) and subjected to single-crystal X-ray diffraction that confirmed the formation of **3**.

Reaction of **5** *with TMSCl.* **5** (0.012 g, 0.015 mmol) was dissolved in $CDCl_3$ (0.7 mL) in an NMR tube, and TMSCl (2 μL, 0.016 mmol) was added. The tube was vigorously shaken for 5 minutes before collecting ^1H and ^{31}P NMR spectra. New resonances at δ 8.32 and 0.06 were observed for $Me_3SiOCHO$ in addition with peaks for $[Au(B_2P_2)]Cl$ and excess TMSCl (δ 0.43). See Figure S13 for the ^1H NMR spectra.

$[Au(B_2P_2)H_2][K(Et_2O)]$ (**6**). **3** (0.034 g, 0.043 mmol) was suspended in Et_2O (4 mL). K[*sec*-Bu_3BH] (89 μL, 2 mol eq, 1.0 M in THF) was then added dropwise, causing the solution to become homogenous briefly before a colorless precipitate appeared. After stirring for 40 minutes, the product was collected via filtration, dissolved in THF (2 x 2 mL), and layered with Et_2O (*ca.* 8 mL). The next day, colorless crystals had appeared from which were separated from the mother liquor and dried *in vacuo*. Yield: 0.028 g, 75%. X-ray quality crystals were grown by layering a concentrated THF solution with Et_2O. ^1H NMR (400 MHz, THF-d_8) δ 7.96 (d, J = 6.6 Hz, 4H), 7.57 (dt, J = 7.4, 3.8 Hz, 4H), 7.27 (t, J = 7.2 Hz, 4H), 7.23 – 7.14 (m, 4H), 6.67 – 6.60 (m, 8H), 6.54 (dd, J = 5.4, 3.3 Hz, 8H), 3.39 (q, J = 7.0 Hz, 4H), 3.27 (q, J = 68.4 Hz, 4H) 2.46 – 2.31 (m, 8H), 1.12 (t, J = 7.0 Hz, 6H), 1.11 (d, J = 7.0 Hz, 12H), 1.06 (d, J = 7.0 Hz, 12H), 0.74 (d, J = 7.0 Hz, 12H), 0.69 (d, J = 7.0 Hz, 12H). $^{31}P\{^1H\}$ NMR (202 MHz, THF-d_8) δ 50.3 (s).^{11}B NMR (160 MHz, THF-d_8) δ −8.66 (d, J = 71.8 Hz). ^{13}C NMR (151 MHz, THF-d_8) δ 174.4, 159.5, 143.8 (t, J = 7.3 Hz), 134.2 (t, J = 25.4 Hz), 133.2, 132.0, 128.9, 124.5, 123.1, 27.8 (t, J = 13.2 Hz), 22.6, 19.8. FTIR: ν_{max} (cm^{-1}) 2089, 1985 (BH). Anal. Calcd for $C_{80}H_{92}Au_2B_4K_2P_4$ (2 x $C_4H_{10}O$): C, 55.06 H, 6.47. Found: C, 55.16 H, 6.26.

$[Au(B_2P_2)(O_2CH)_2][K(18\text{-}c\text{-}6)]$ (7). A THF (3 mL) solution of **6** (0.020 g, 0.012 mmol) and 18-crown-6 (0.003 g, 0.013 mmol) was subjected to three freeze-pump-thaw cycles. 1 atm CO_2 was added and the reaction was stirred 15 minutes before removing volatiles *in vacuo*. The product was rinsed with hexanes (1 mL) and Et_2O (1 mL) before being dried *in vacuo*. Yield: 0.012 g, 87%. X-ray quality crystals were grown by layering a concentrated benzene solution with hexanes. ^1H NMR (500 MHz, C_6D_6) δ 8.69 (d, J = 7.5 Hz, 2H), 8.34 (s, 2H), 7.58 (t, J = 7.4 Hz, 2H), 7.43 (s, 2H), 7.32 (t, J = 7.4 Hz, 2H), 7.26 – 7.19 (m, 4H), 7.07 – 6.99 (m, 4H), 3.27 (s, 24H), 2.23 (m, 4H), δ 0.94 (q, J = 7.4 Hz, 12H), 0.75 (q, J = 8.1 Hz, 12H).$^{31}P\{^1H\}$ NMR (202 MHz, C_6D_6) δ 46.4 (s). $^{11}B\{^1H\}$ (160 MHz, C_6D_6) δ 1.83 (bs). ^{13}C NMR (151 MHz, C_6D_6) δ 169.0, 168.7, 155.0, 136.0 (t, J = 6.1 Hz), 134.9 (t, J = 25.5 Hz), 134.4, 131.5, 129.2, 125.1, 124.5, 26.8 (t, J = 13.0 Hz), 22.4, 18.9. FTIR: ν_{max} (cm^{-1}) 1678 (C=O). Anal. Calcd for $C_{50}H_{70}AuB_2KO_{10}P_2$ (1x C_6H_{14}): C, 54.38 H, 6.85. Found: C, 53.92 H, 6.94.

$[Au(B_2P_2)(CO_3)][K(18\text{-}c\text{-}6)]$ (8). A solution of **1** (0.015 g, 0.014 mmol) in benzene (4 mL) was subjected to three freeze-pump-thaw cycles before adding 1 atm CO_2. The reaction was stirred 15 minutes before removing volatiles *in vacuo* to yield a colorless solid. Yield: 0.14 g, 89%. X-ray quality crystals were grown over the course of two days by letting the reaction mixture stand in benzene under a CO_2 atmosphere. ^1H NMR (500 MHz, C_6D_6) δ 8.65 (d, J = 8.6 Hz, 2H), 7.66 (t, J = 7.2 Hz, 2H), 7.50 (dt, J = 7.7, 3.9 Hz, 2H), 7.39 (t, J = 7.3 Hz, 2H), 7.07 (dd, J = 5.2, 3.3 Hz, 4H), 7.01 (dd, J = 5.1, 3.4 Hz, 4H), 3.20 (s, 24H), 2.45 – 2.37 (m, 4H), 1.02 (d, J = 7.0 Hz, 6H), 0.99 (d, J = 7.0 Hz, 6H), 0.85 (d, J = 7.9 Hz, 6H), 0.82 (d, J = 7.8 Hz, 6H). ^{31}P NMR (202 MHz, C_6D_6) δ 43.59. $^{11}B\{^1H\}$ (242 MHz, C_6D_6) δ 0.83 (bs). ^{13}C NMR (126 MHz, C_6D_6) δ 168.0, 158.6, 155.3, 136.3 (t, $J = 25.4$ Hz), 133.3 (t, $J = 5.8$ Hz), 131.6, 130.5, 128.6, 124.9, 123.8, 70.3, 26.0 (t, $J = 12.3$ Hz), 23.2, 18.8. FTIR: $\nu_{\max}$ 1592 cm^{-1} (C=O). This compound is unstable in solution in the absence of CO_2, and despite numerous attempts, satisfactory elemental analysis of this compound could not obtained.

[Au(B_2P_2)]($^{13}CO_3$)][K(18-c-6)] (8-^{13}C). The ^{13}C-labeled compound was synthesized similarly to **8** using $^{13}CO_2$. ^{1}H, ^{31}P and ^{11}B NMR were identical to **8**. The isotopically enriched carbon appears at 168.9 ppm in the ^{13}C NMR spectrum. ^{1}H NMR (600 MHz, C_6D_6) δ 8.65 (d, $J = 7.1$ Hz, 2H), 7.67 (t, $J = 7.2$ Hz, 2H), 7.50 (s, 2H), 7.40 (t, $J = 7.5$ Hz, 2H), 7.09 – 7.05 (m, 4H), 7.04 – 6.99 (m, 4H), 3.20 (s, 18H), 2.41 (s, 4H), 1.02 (d, $J = 6.9$ Hz, 6H), 1.00 (d, $J = 7.0$ Hz, 6H), 0.85 (d, $J = 8.0$ Hz, 6H), 0.82 (d, $J = 8.3$ Hz, 6H). ^{13}C NMR (151 MHz, C_6D_6) δ 168.9, 158.6, 158.2, 155.3, 136.3 (t, $J = 25.0$ Hz), 133.3, 131.6, 130.5, 129.0 – 128.5 (m), 124.8, 123.8, 70.2, 26.0 (t, $J = 12.2$ Hz), 23.2, 18.8. FTIR: $\nu_{\max}$ 1549 cm^{-1} (C=O).

Au(B_2P_2)(OSi^{i}Pr$_3$) (9). **1** (0.015 g, 0.014 mmol) was dissolved in benzene (5 mL) and cooled to –196 °C prior to adding triisopropylsilyl chloride (0.003 g, 0.015 mmol) as a benzene (1 mL) solution. The mixture was briefly thawed, gently stirred to ensure homogeneity, and then subjected to three freeze-pump-thaw cycles prior to introducing 1 atm CO_2. The reaction immediately turned yellow, and after 15 minutes, the volatiles were removed *in vacuo*. The resulting yellow foam was washed with hexanes (3 x 1 mL), dissolved in toluene (2 x 1 mL), filtered through celite, layered with HMDSO (2 mL), and let stand overnight. The next day, the pale-yellow crystalline product was rinsed with hexanes (1 x1 mL) and dried *in vacuo*. Yield: 0.010 g, 73%. X-ray quality crystals were grown by layering a concentrated toluene solution with HMDSO. ^{1}H NMR (500 MHz, C_6D_6) δ 9.61 (ddd, $J = 7.5$, 4.1, 1.2 Hz, 1H), 8.06 (d, $J = 7.4$ Hz, 1H), 7.84 (t, $J = 7.4$ Hz, 1H), 7.58 (d, $J = 7.4$ Hz, 2H), 7.41 (t, $J = 8.5$ Hz, 1H), 7.29 (t, $J = 7.5$ Hz, 1H), 7.27 (d, $J = 7.1$ Hz, 2H), 7.25 – 7.19 (m, 2H), 7.17–7.14 (m, 2H), 7.12 (t, $J = 7.6$ Hz, 1H), 6.94 (t, $J = 7.3$ Hz, 2H), 1.96 (tdd, $J = 13.6$, 7.7, 1.7 Hz, 4H), 1.20 (d, $J = 7.4$ Hz, 18H), 1.04 (dq, $J = 15.1$, 7.2 Hz, 3H), 0.75 (d, $J = 6.9$ Hz, 4H), 0.71 (d, $J = 7.0$ Hz, 4H), 0.68 (d, $J = 6.9$ Hz, 2H), 0.65 (d, $J = 6.9$ Hz, 2H), 0.49 (d, $J = 7.0$ Hz, 2H), 0.46 (d, $J = 7.0$ Hz, 2H). ^{31}P NMR (202 MHz, C_6D_6) δ 56.0 (d, $J = 240.0$ Hz), 52.5 (d, $J = 239.9$ Hz). ^{11}B NMR (160 MHz, C_6D_6) δ 51.5, –3.0. ^{13}C NMR (126 MHz, C_6D_6) δ 173.1, 170.7, 159.2 (d, $J = 29.8$ Hz), 140.7, 137.7 (d, $J = 14.2$ Hz), 137.4 (dd, $J = 15.1$, 9.0 Hz), 136.1 (d, $J = 10.6$ Hz), 135.2 (d, $J = 9.4$ Hz), 134.9 (d, $J = 8.8$ Hz), 132.3 (d, $J = 13.6$ Hz), 131.5 (t, $J = 14.8$ Hz), 131.1, 131.0, 129.8, 129.5 (d, $J = 6.9$ Hz), 129.1 (d, $J = 6.8$ Hz), 126.7, 124.3 (d, $J = 8.7$ Hz), 29.2, 29.0, 27.8, 27.6, 20.7, 20.2, 19.6, 14.3. MALDI MS: m/z 930.4087; Calcd. 930.4132.

Spectroscopic Data

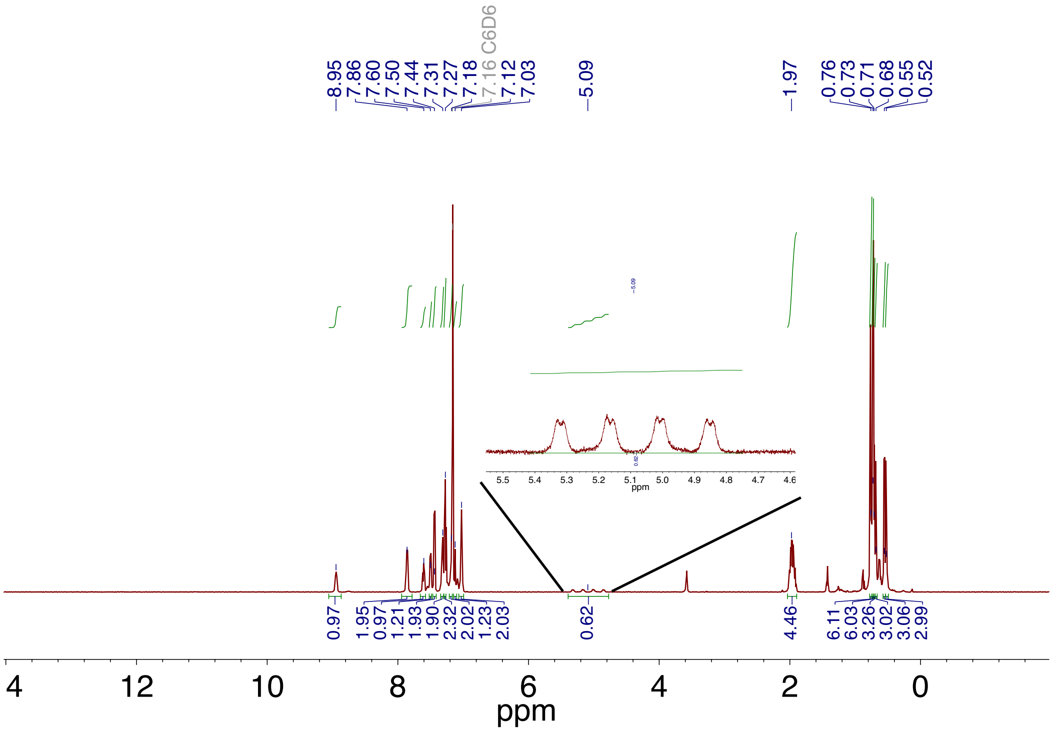

Figure S1. ^{1}H NMR spectrum of [Au(B_2P_2)]H (**2**) recorded at 500 MHz in C_6D_6.

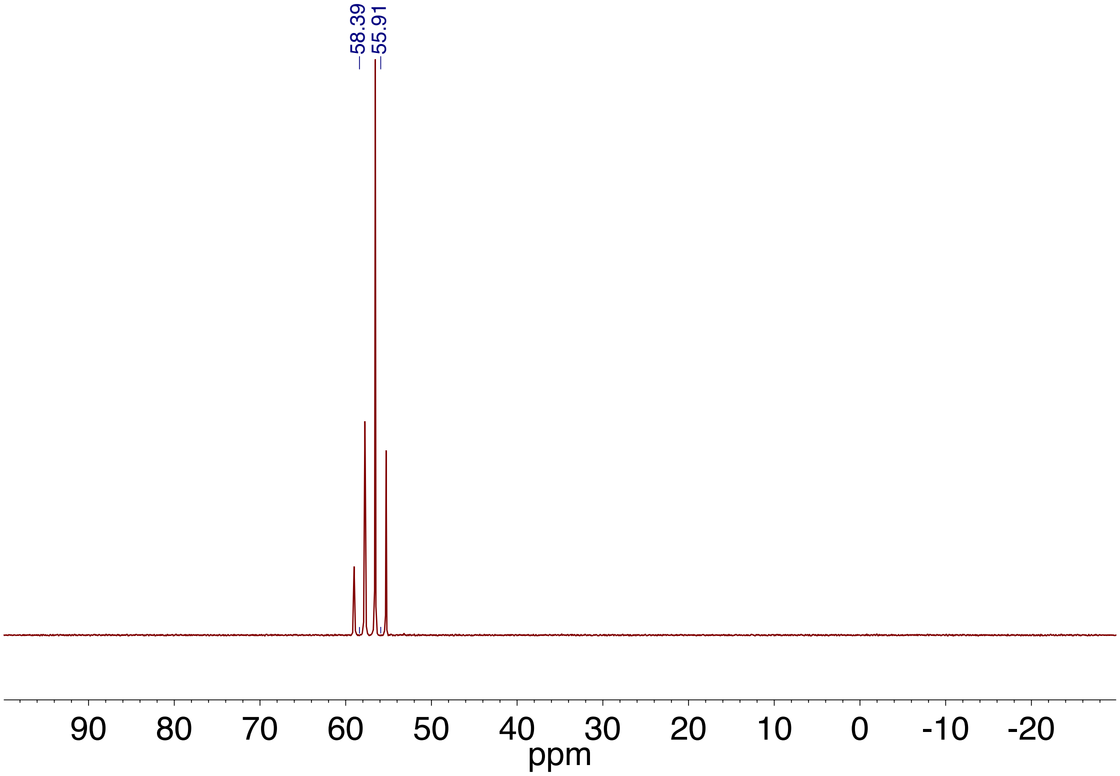

Figure S2. ^{31}P NMR spectrum of [Au(B_2P_2)]H (**2**) recorded at 202 MHz in C_6D_6.

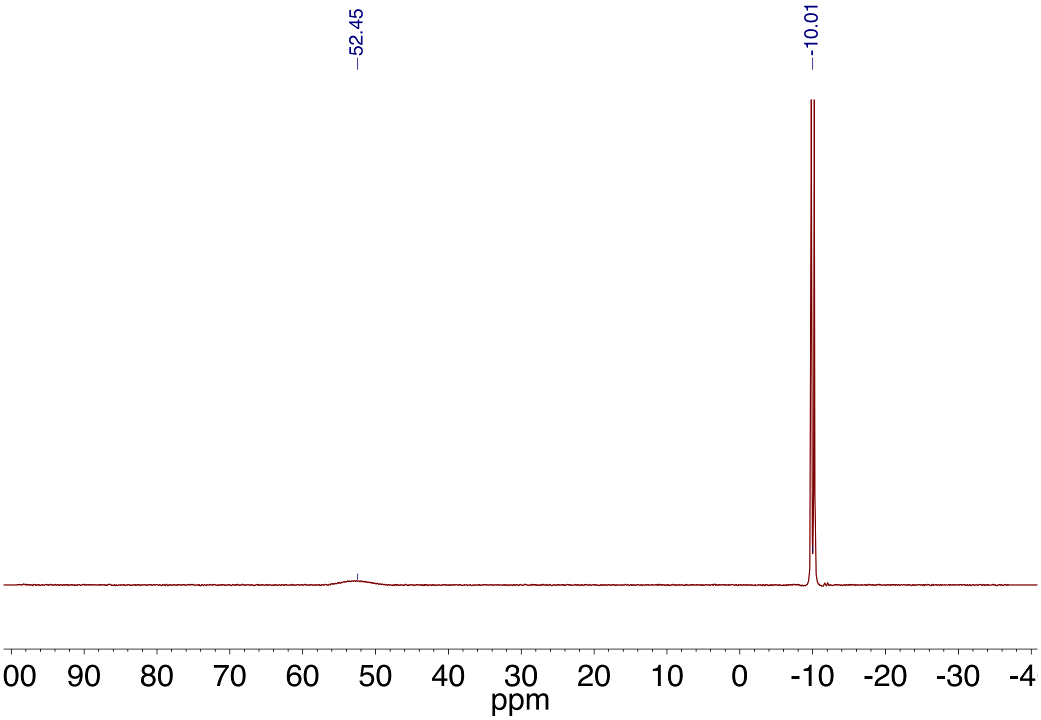

Figure S3. ^{11}B NMR spectrum of [Au(B_2P_2)]H (**2**) recorded at 160 MHz in THF:C_6D_6 (1:1).

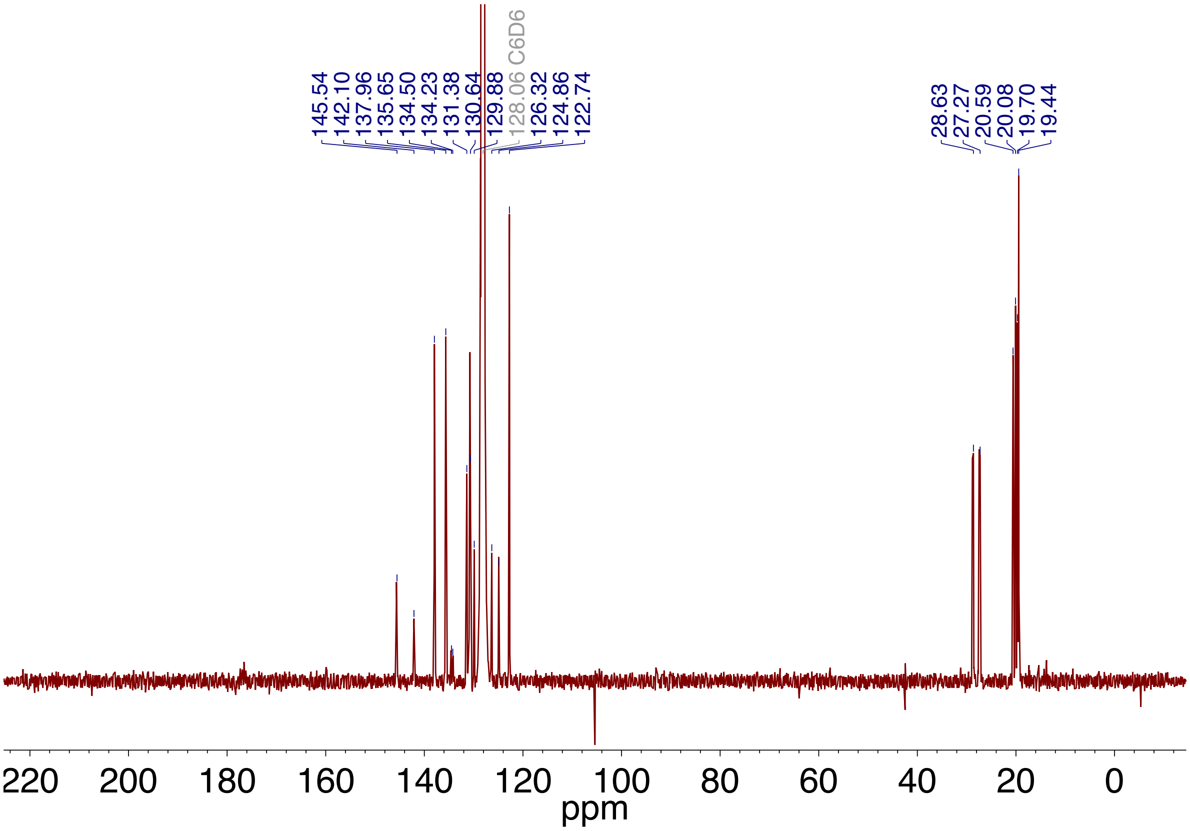

Figure S4. ^{13}C{^{1}H} NMR spectrum of [Au(B_2P_2)]H (**2**) recorded at 126 MHz in C_6D_6.

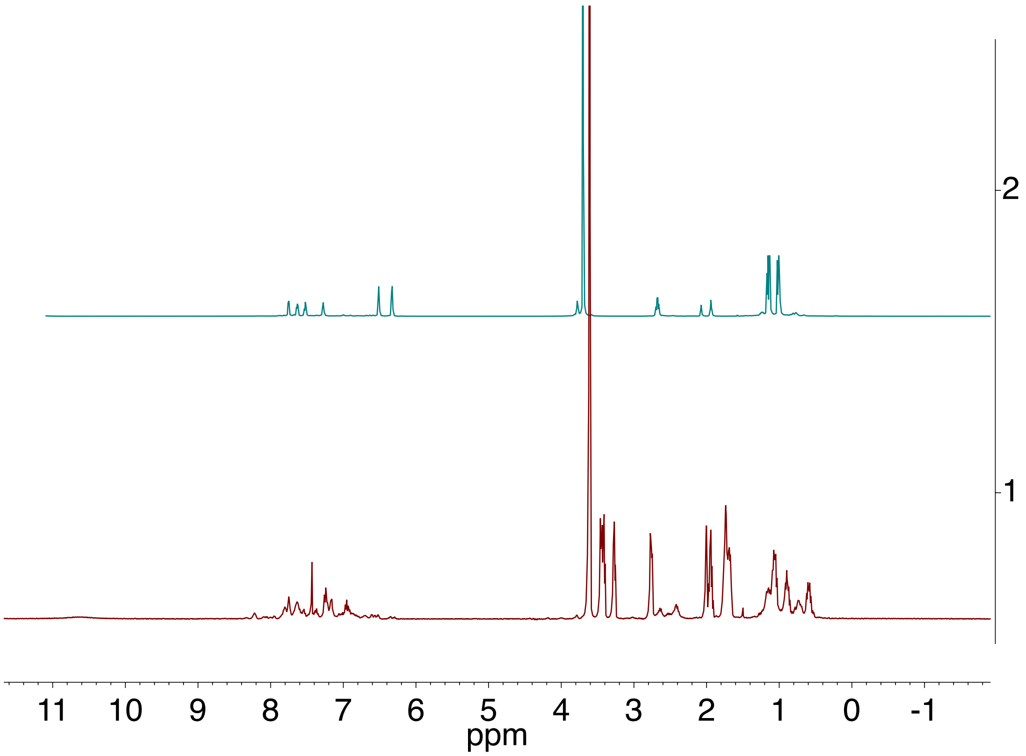

Figure S5. ^{1}H NMR spectra before (**cyan**) and after addition (**red**) of DBU•HCl to [Au(B_2P_2)][K(18-c-6)] (**1**) recorded at 500 MHz in CD_3CN.

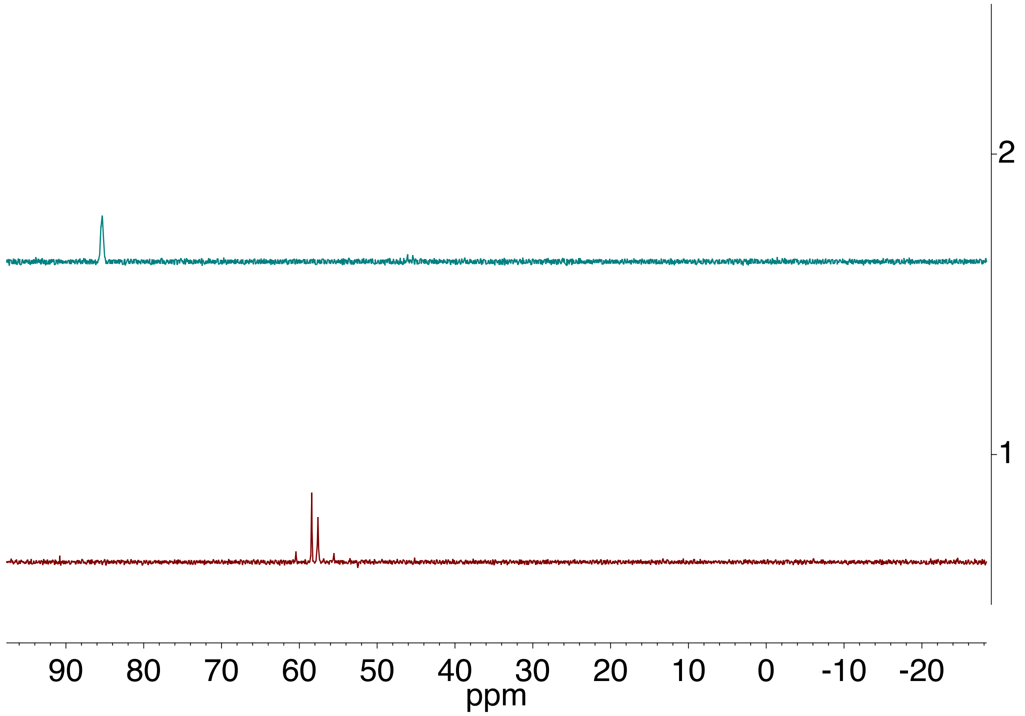

Figure S6. ^{31}P NMR spectra before (**cyan**) and after addition (**red**) of DBU•HCl to [Au(B_2P_2)][K(18-c-6)] (**1**) recorded at 500 MHz in CD_3CN.

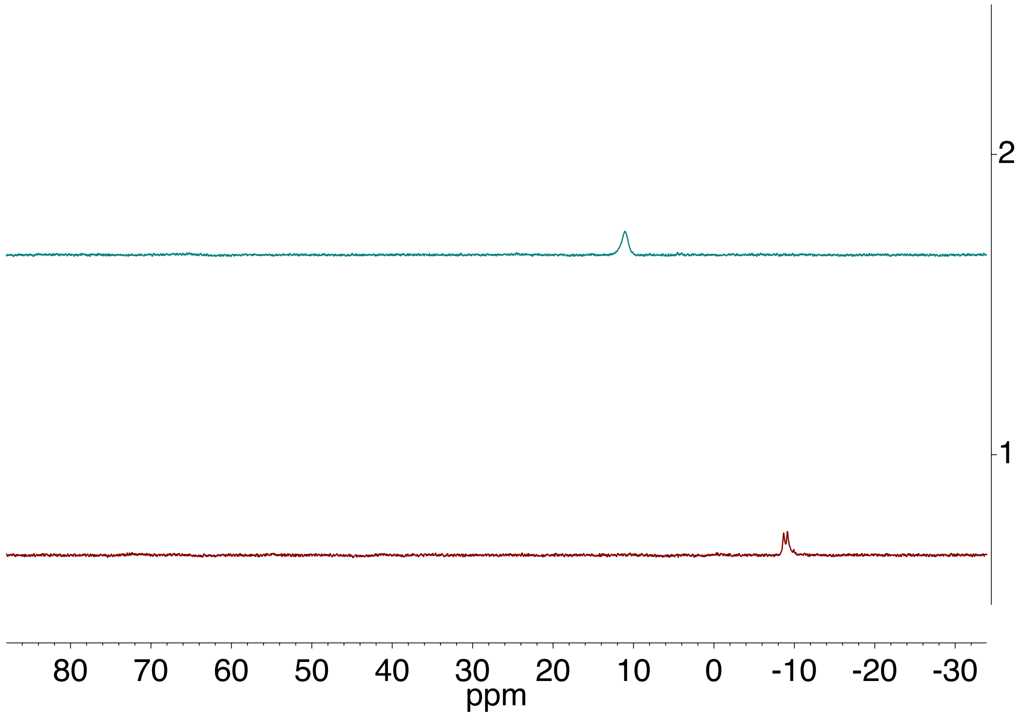

Figure S7. ^{11}B NMR spectra before (**cyan**) and after addition (**red**) of DBU•HCl to [Au(B_2P_2)][K(18-c-6)] (**1**) recorded at 500 MHz in CD_3CN.

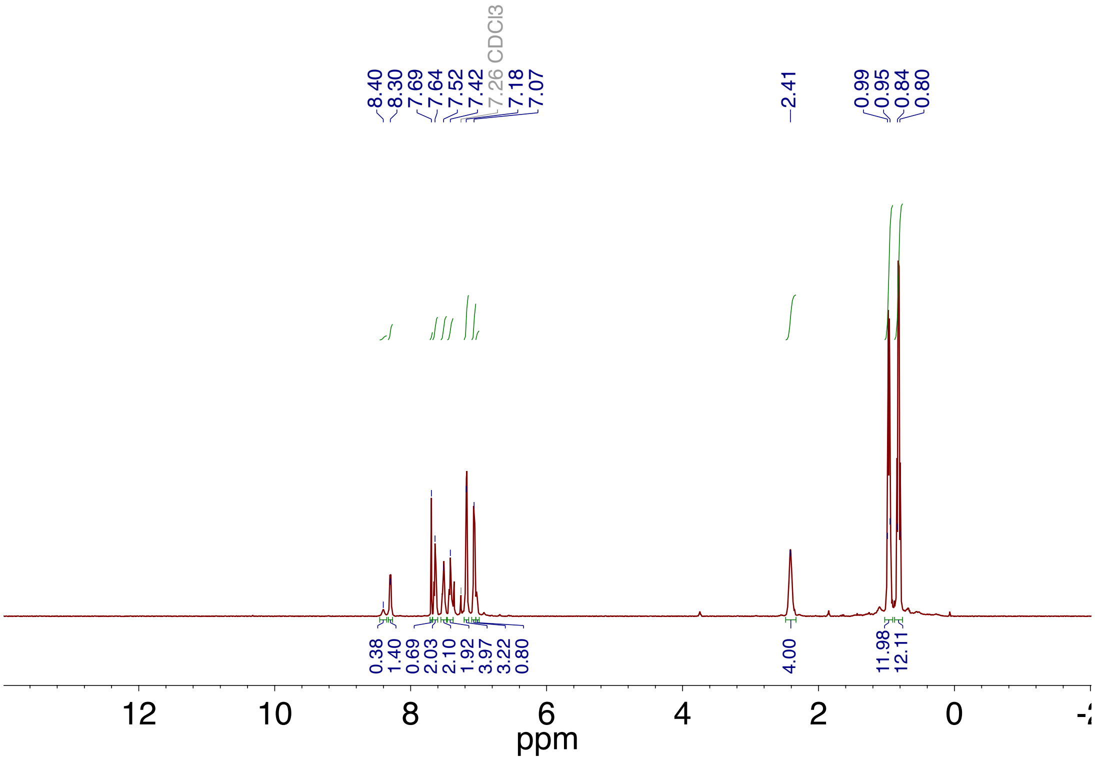

Figure S8. ^{1}H NMR spectrum of Au(B_2P_2)(CO_2H) (**5**) recorded at 500 MHz in $CDCl_3$.

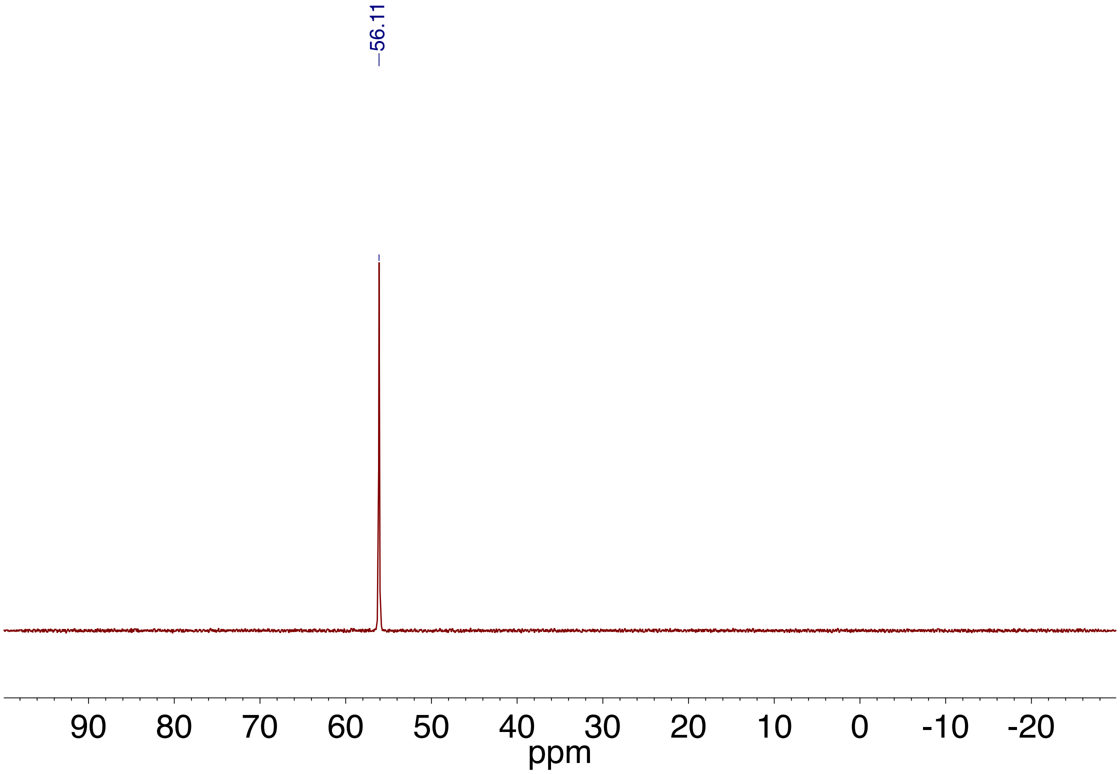

Figure S9. ^{31}P NMR spectrum of Au(B_2P_2)(CO_2H) (**5**) recorded at 202 MHz in $CDCl_3$.

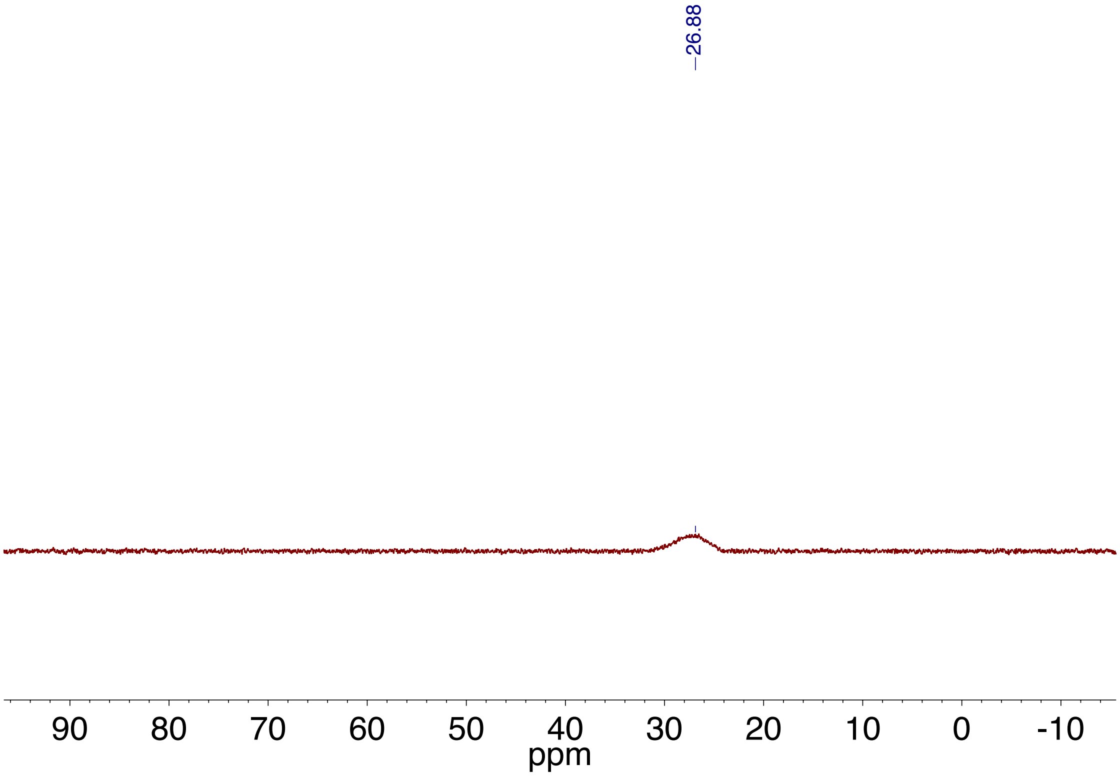

Figure S10. ^{11}B NMR spectrum of Au(B_2P_2)(CO_2H) (**5**) recorded at 193 MHz in $CDCl_3$.

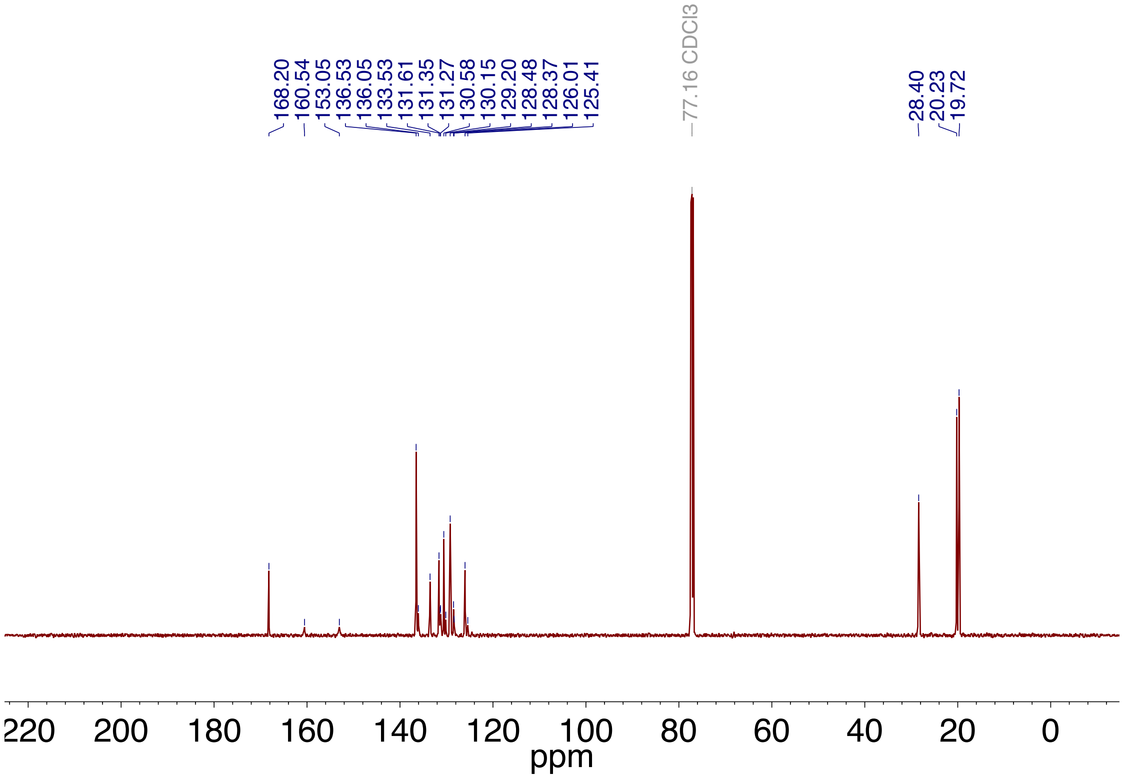

Figure S11. $^{13}C\{^{1}H\}$ NMR spectrum of $Au(B_2P_2)(CO_2H)$ (**5**) recorded at 126 MHz in $CDCl_3$.

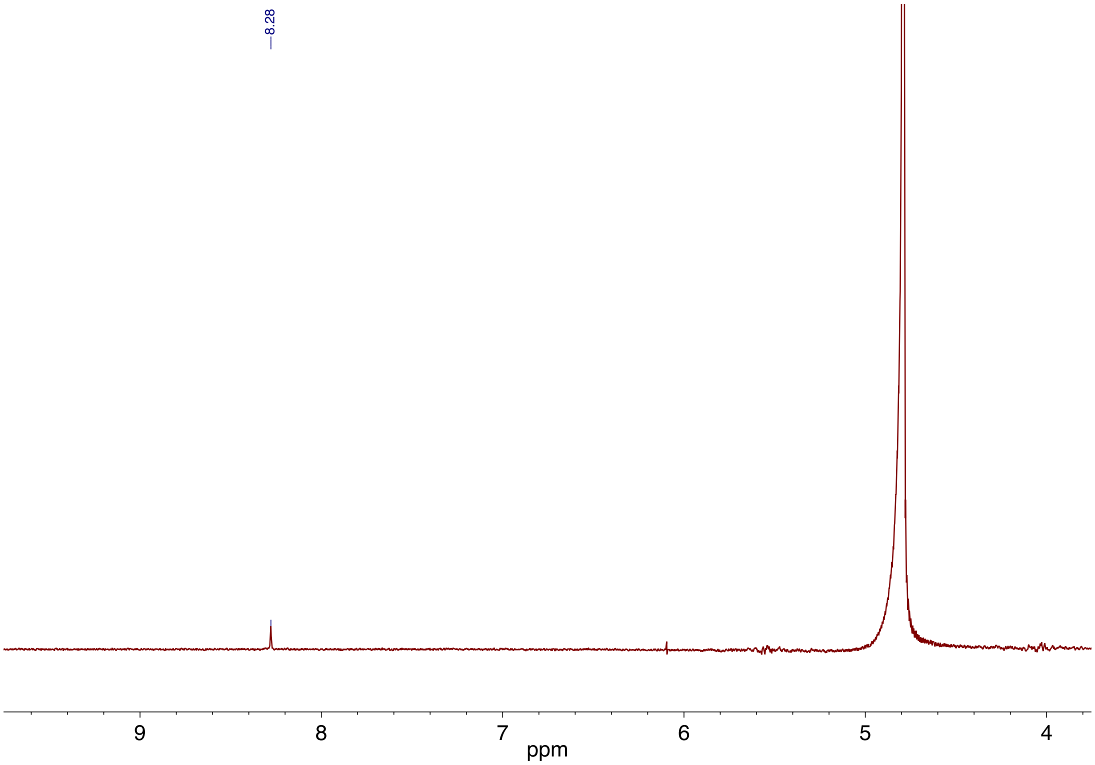

Figure S12. ^{1}H NMR spectrum of the filtered solid after the reaction of $Au(B_2P_2)(CO_2H)$ (**5**) with $Na(C_{10}H_8)$ recorded at 500 MHz in D_2O.

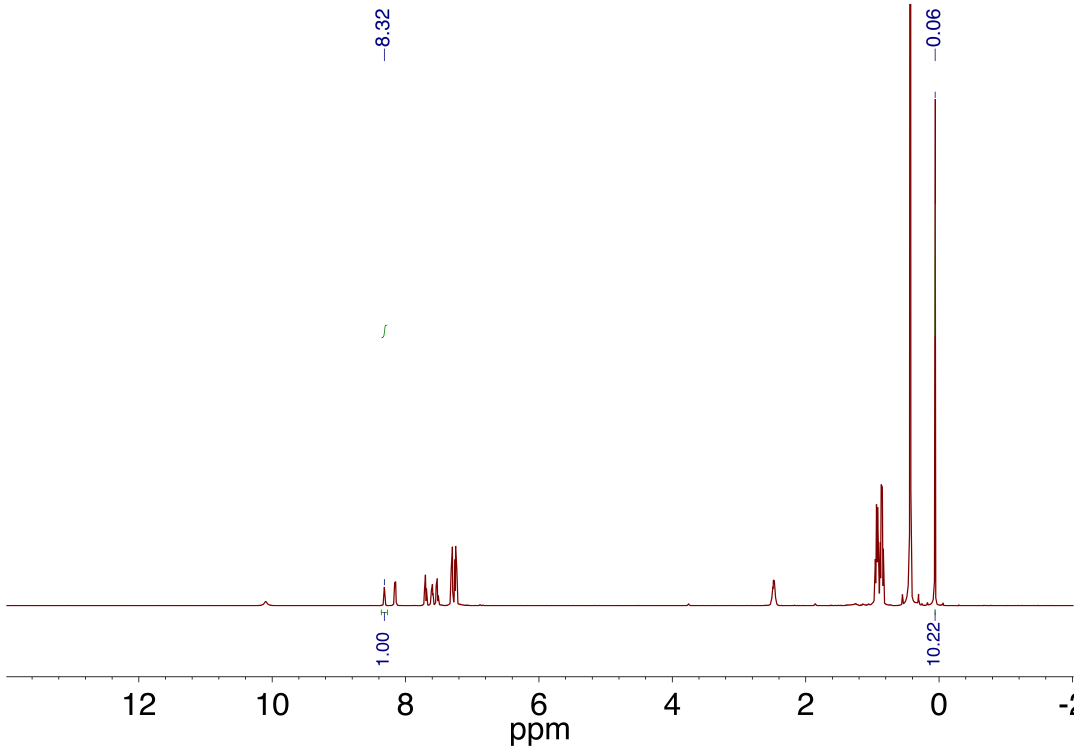

Figure S13. ^{1}H NMR spectrum after the reaction of Au(B_2P_2)(CO_2H) (**5**) with TMSCl recorded at 500 MHz in $CDCl_3$. Selected peaks are for TMS-OCHO.

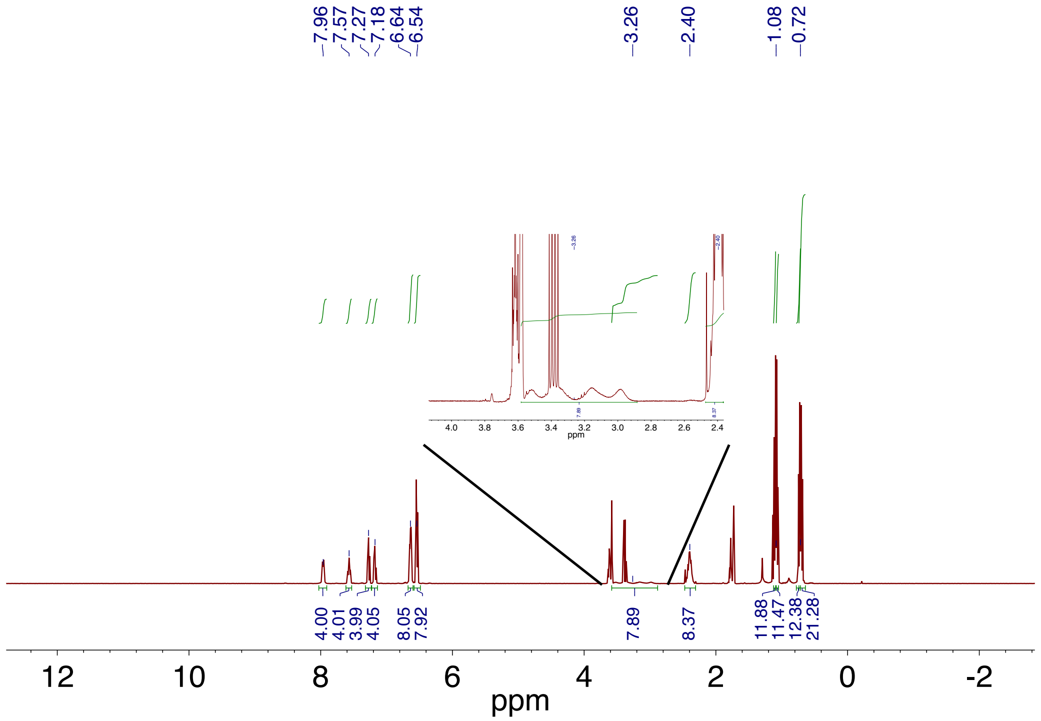

Figure S14. ^{1}H NMR spectrum of [Au(B_2P_2)H_2][K(Et_2O)] (**6**) recorded at 400 MHz in THF-d_8.

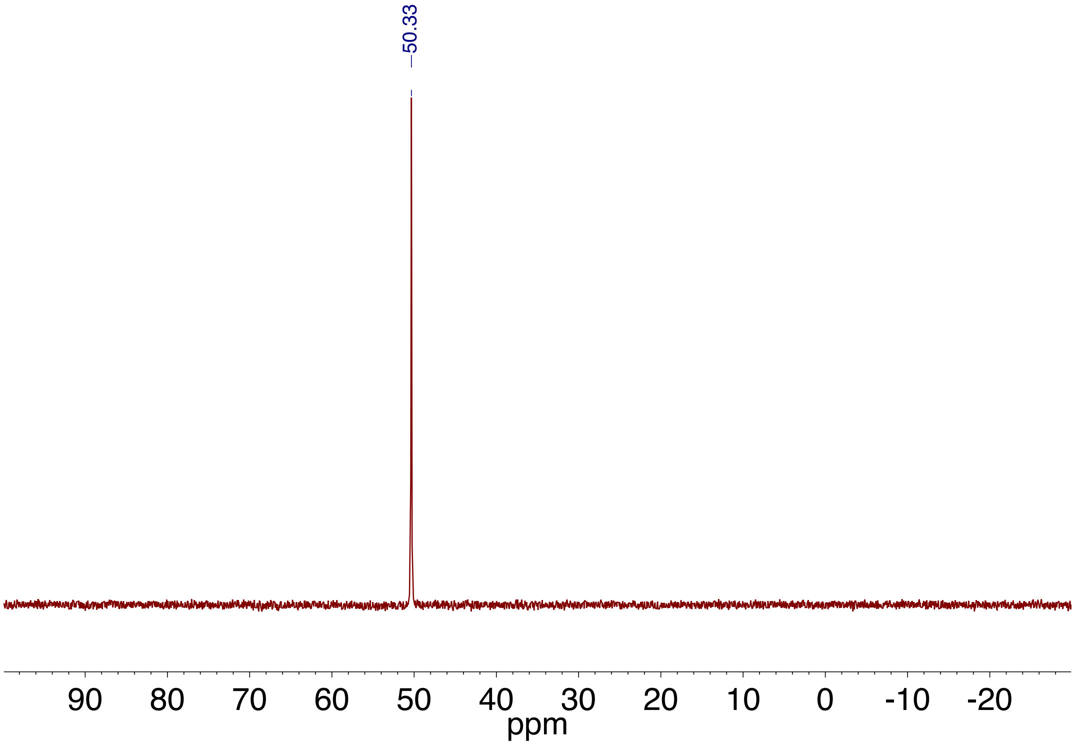

Figure S15. ^{31}P NMR spectrum of $[Au(B_2P_2)(H_2)][K(Et_2O)]$ (**6**) recorded at 162 MHz in THF-d_8.

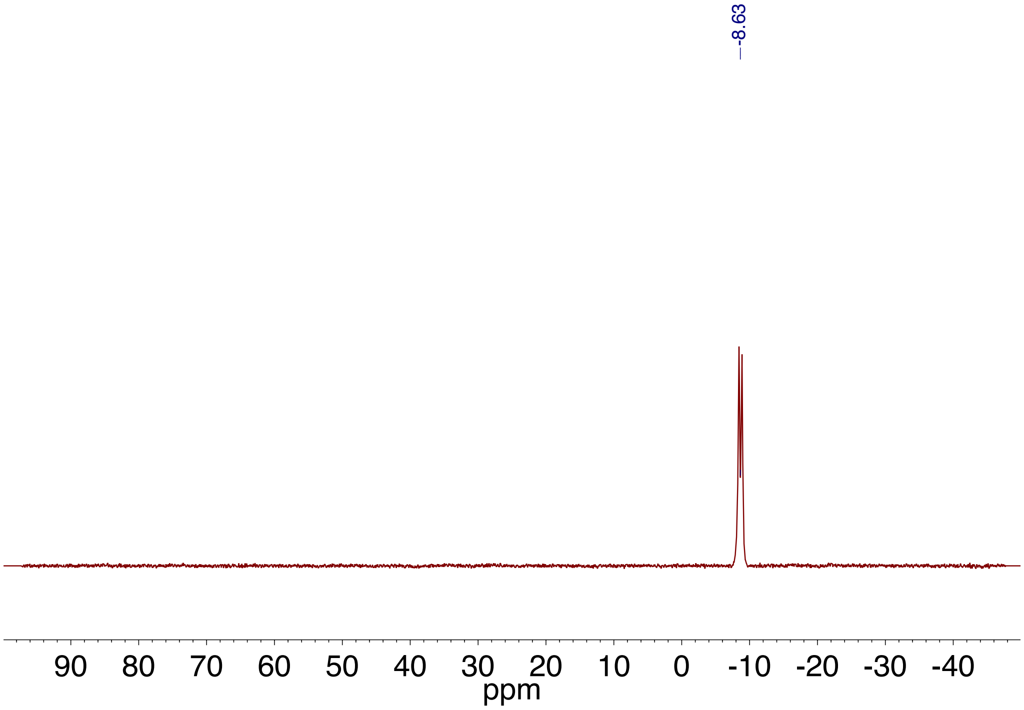

Figure S16. ^{11}B NMR spectrum of $[Au(B_2P_2)(H_2)][K(Et_2O)]$ (**6**) recorded at 128 MHz in THF-d_8.

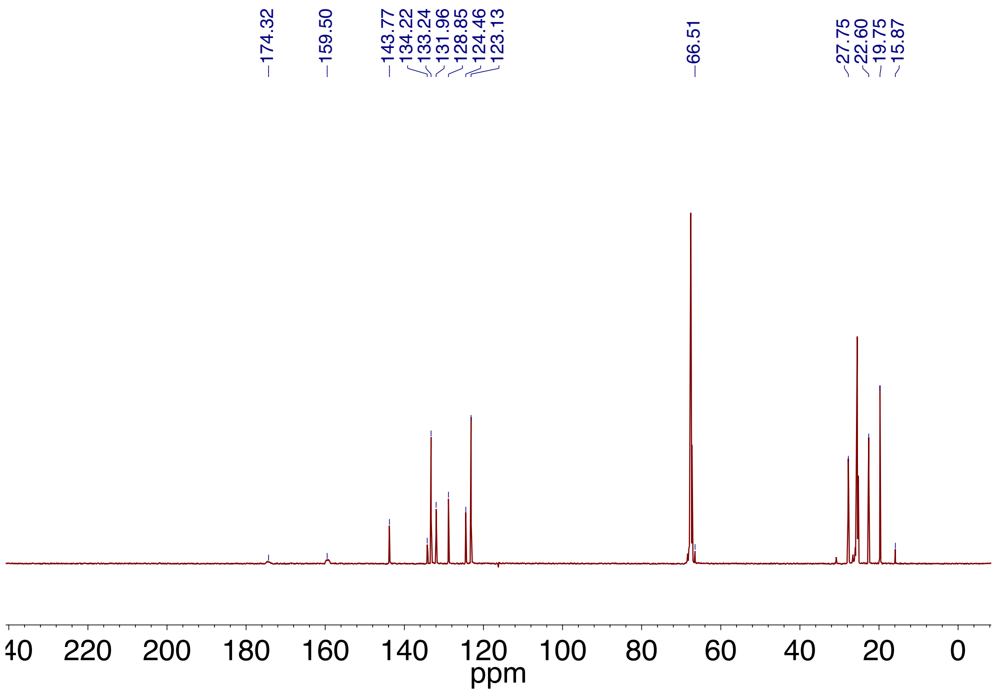

Figure S17. $^{13}C\{^{1}H\}$ NMR spectrum of $[Au(B_2P_2)(H_2)][K(Et_2O)]$ (**6**) recorded at 101 MHz in THF-d_8.

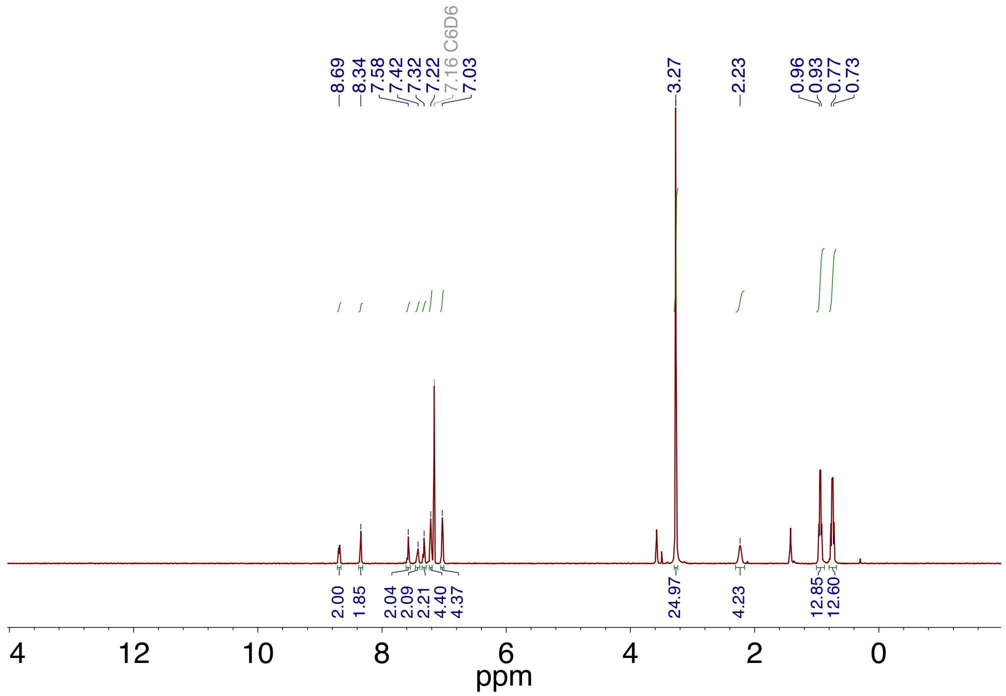

Figure S18. ^{1}H NMR spectrum of $[Au(B_2P_2)(CO_2H)_2][K(18\text{-}c\text{-}6)]$ (**7**) recorded at 500 MHz in C_6D_6.

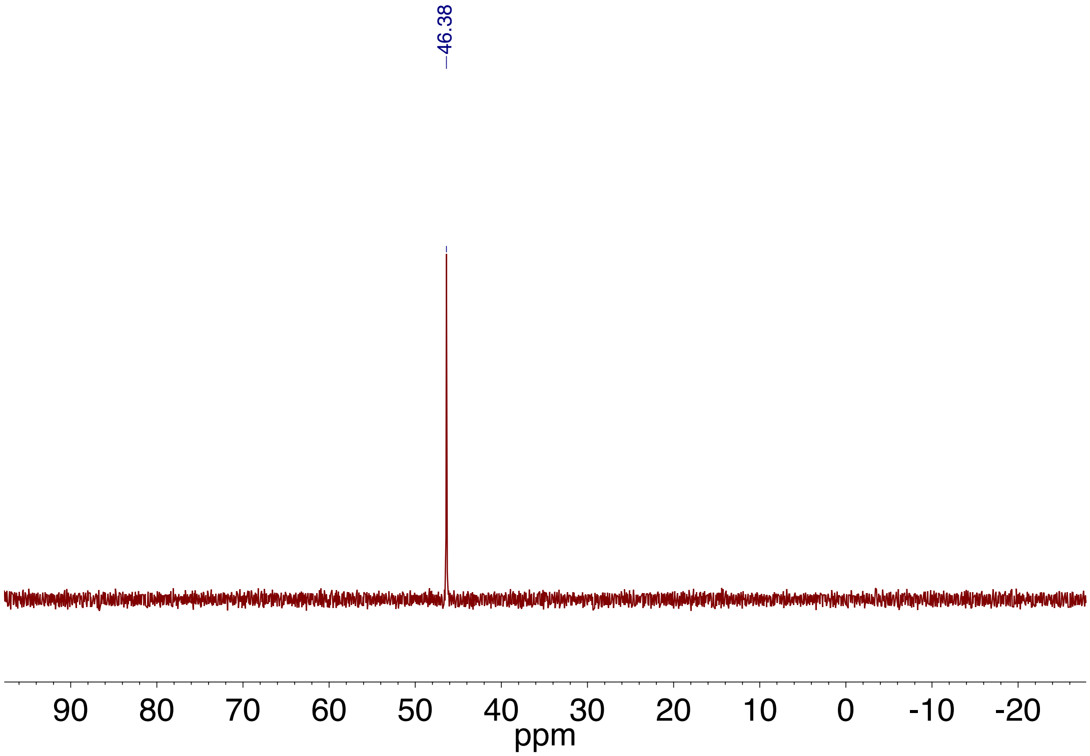

Figure S19. ^{31}P NMR spectrum of [Au(B_2P_2)(CO_2H)$_2$][K(18-c-6)] (**7**) recorded at 162 MHz in C_6D_6.

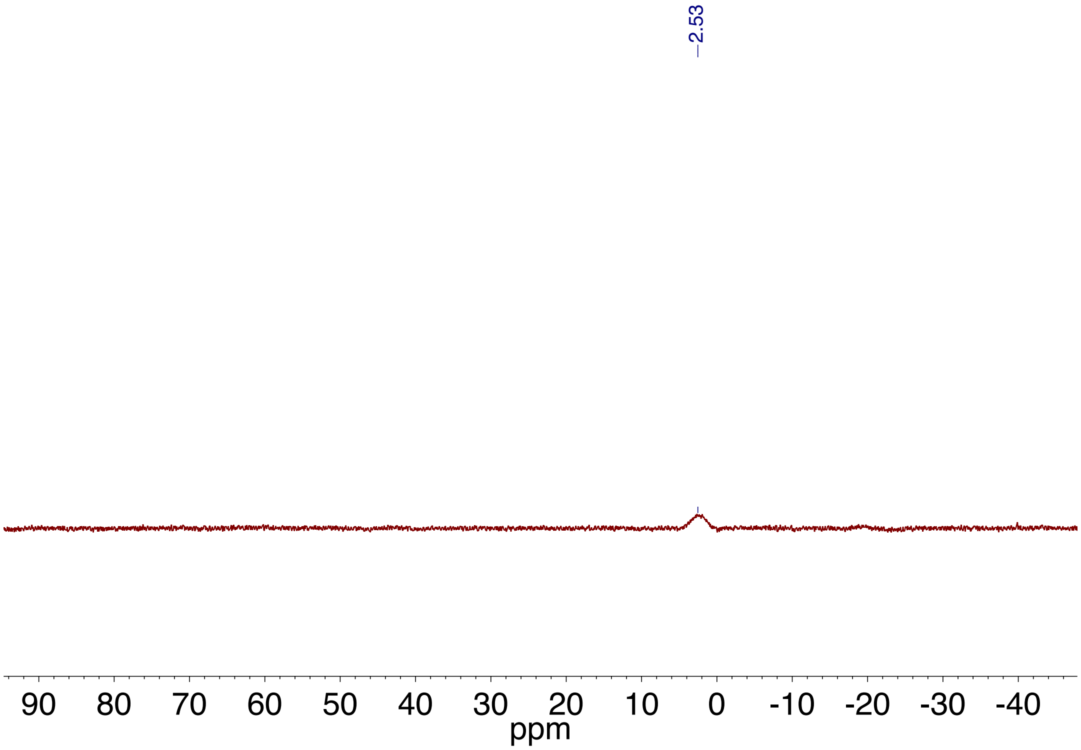

Figure S20. ^{11}B NMR spectrum of [Au(B_2P_2)(CO_2H)$_2$][K(18-c-6)] (**7**) recorded at 128 MHz in C_6D_6.

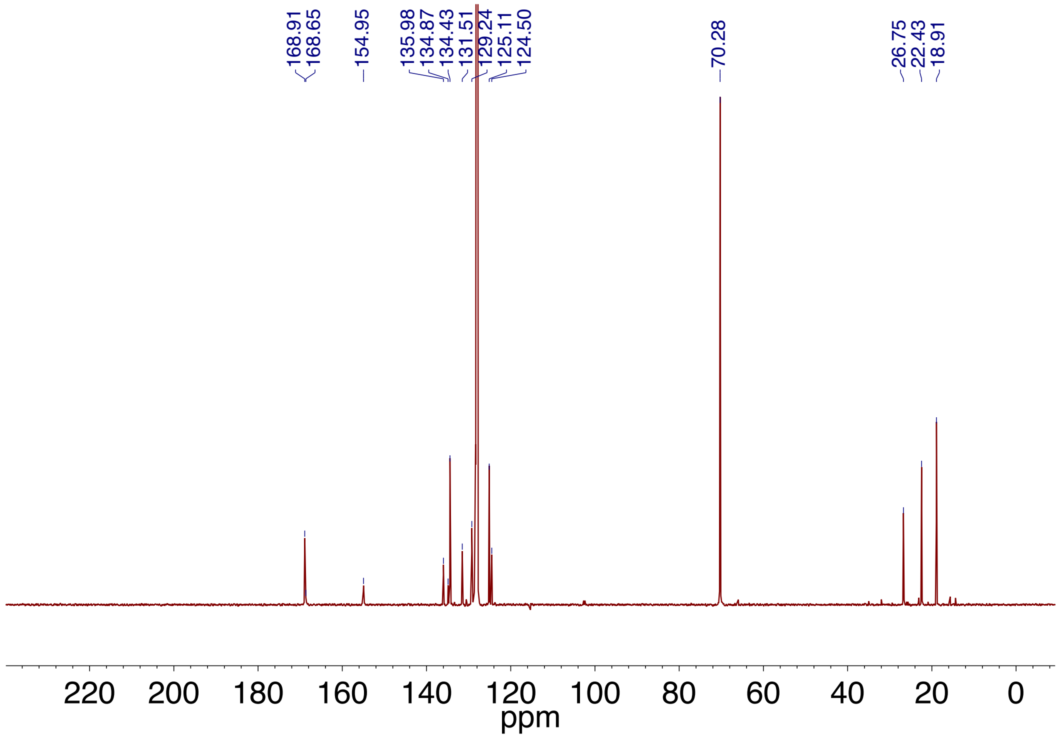

Figure S21. $^{13}C\{^1H\}$ NMR spectrum of [Au(B_2P_2)(CO_2H)$_2$][K(18-c-6)] (**7**) recorded at 101 MHz in C_6D_6.

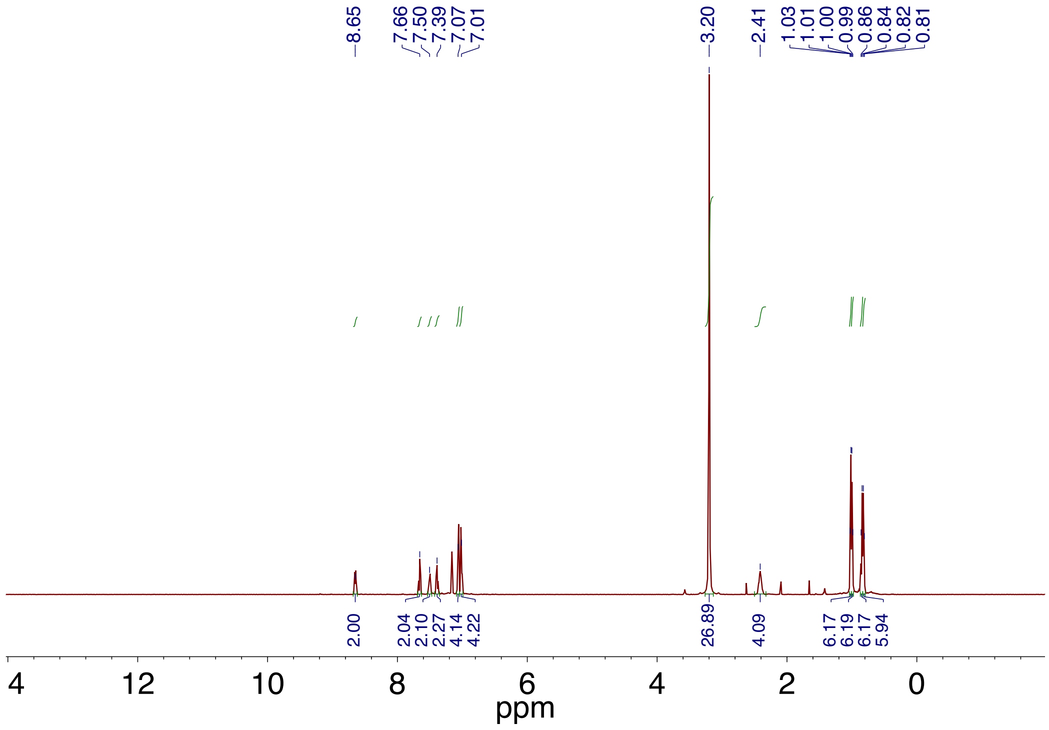

Figure S22. ^1H NMR spectrum of [Au(B_2P_2)(CO_2H)$_2$][K(18-c-6)] (**7**) recorded at 500 MHz in C_6D_6.

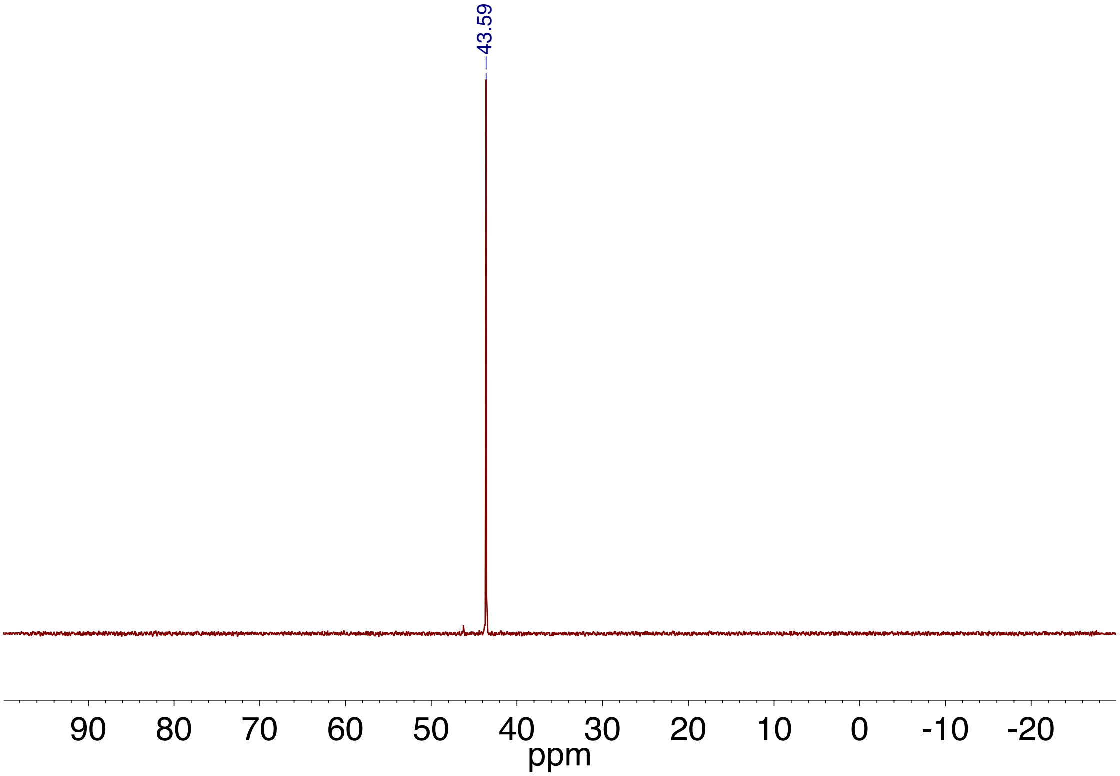

Figure S23. ^{31}P NMR spectrum of [Au(B_2P_2)(CO_3)][K(18-c-6)] (**8**) recorded at 202 MHz in C_6D_6.

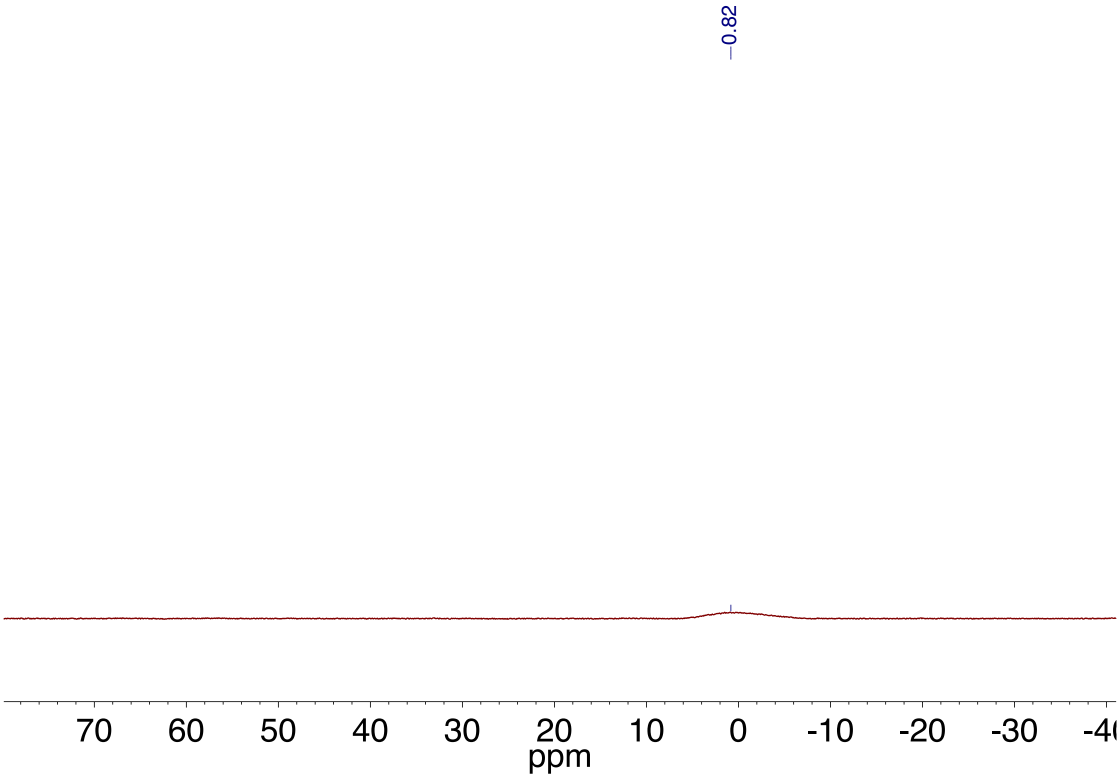

Figure S24. ^{11}B NMR spectrum of [Au(B_2P_2)(CO_3)][K(18-c-6)] (**8**) recorded at 242 MHz in C_6D_6.

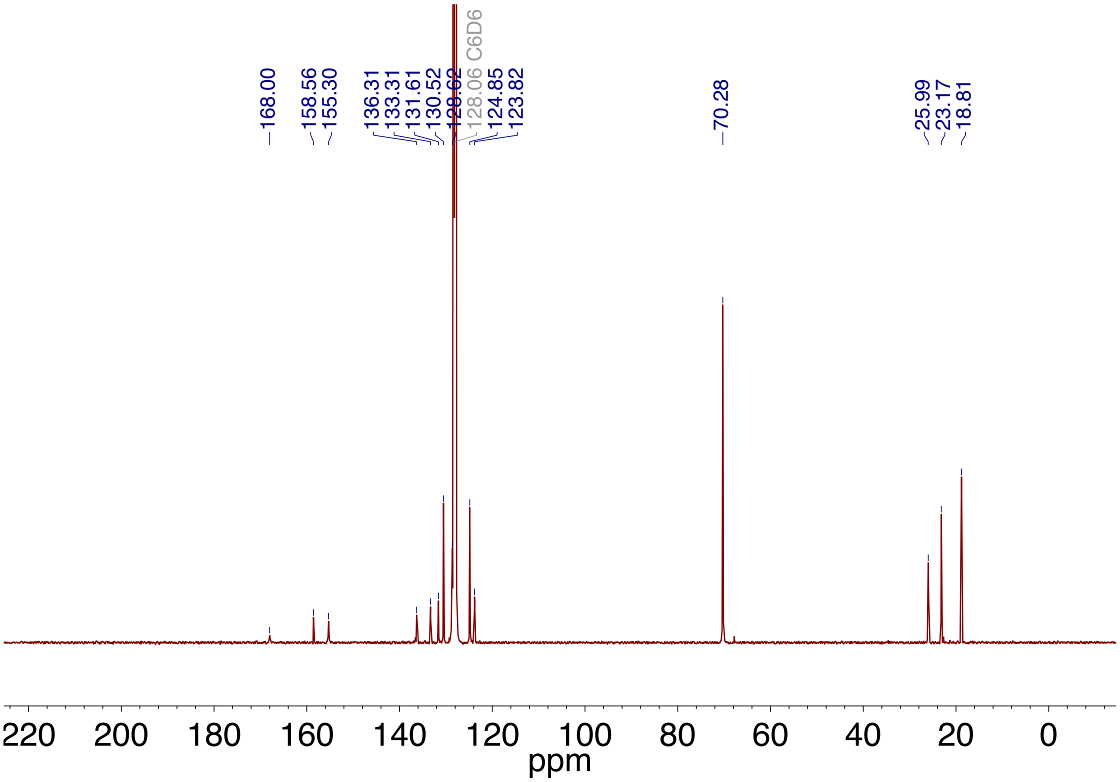

Figure S25. $^{13}C\{^{1}H\}$ NMR spectrum of [Au(B_2P_2)(CO_3)][K(18-c-6)] (**8**) recorded at 126 MHz in C_6D_6.

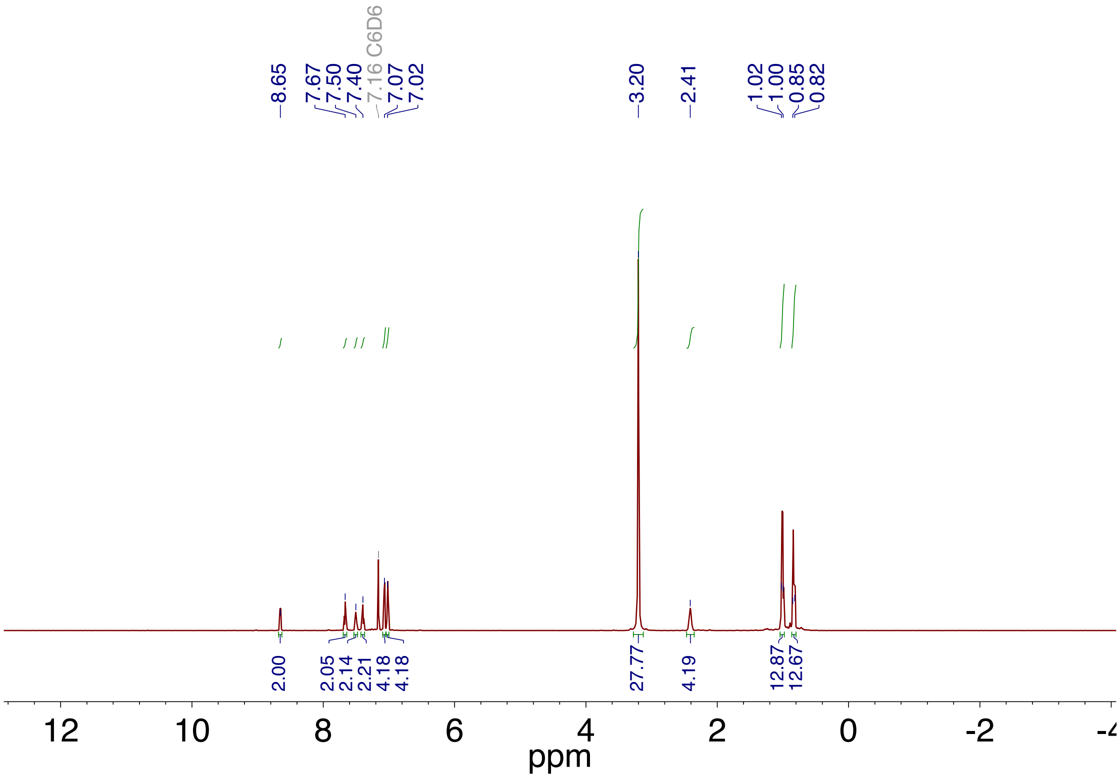

Figure S26. ^{1}H NMR spectrum of [Au(B_2P_2)($^{13}CO_3$)][K(18-c-6)] (**8-^{13}C**) recorded at 500 MHz in C_6D_6.

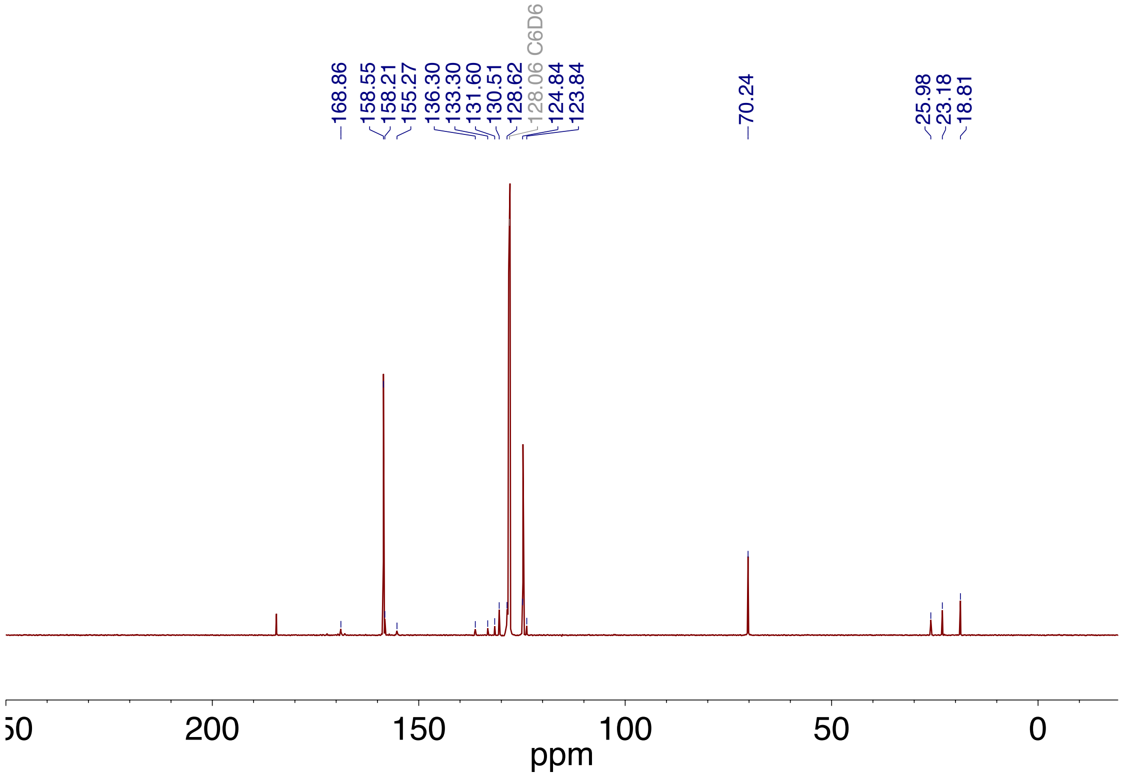

Figure S27. ^{13}C{^{1}H} NMR spectrum of [Au(B$_2$P$_2$)(^{13}CO$_3$)][K(18-c-6)] (**8-^{13}C**) recorded at 126 MHz in C$_6$D$_6$.

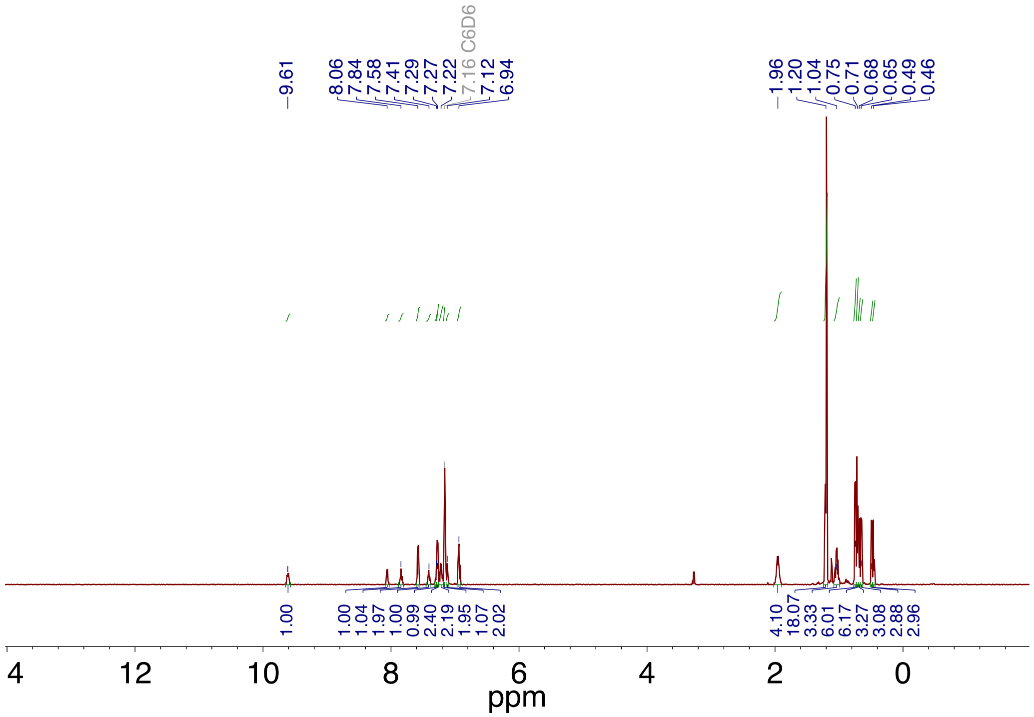

Figure S28. ^{1}H NMR spectrum of [Au(B$_2$P$_2$)](O(Si^{i}Pr$_3$) (**9**) recorded at 500 MHz in C$_6$D$_6$.

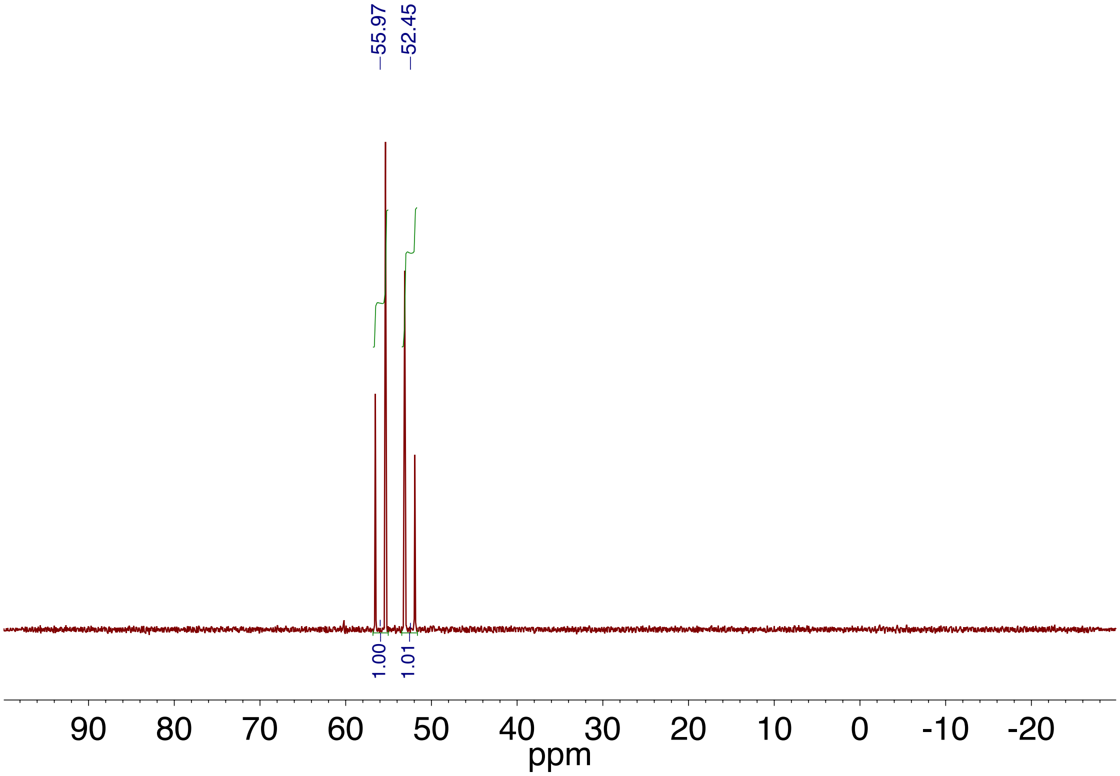

Figure S29. ^{31}P NMR spectrum of [Au(B$_2$P$_2$)](O(Si^{i}Pr$_3$) (**9**) recorded at 202 MHz in C$_6$D$_6$.

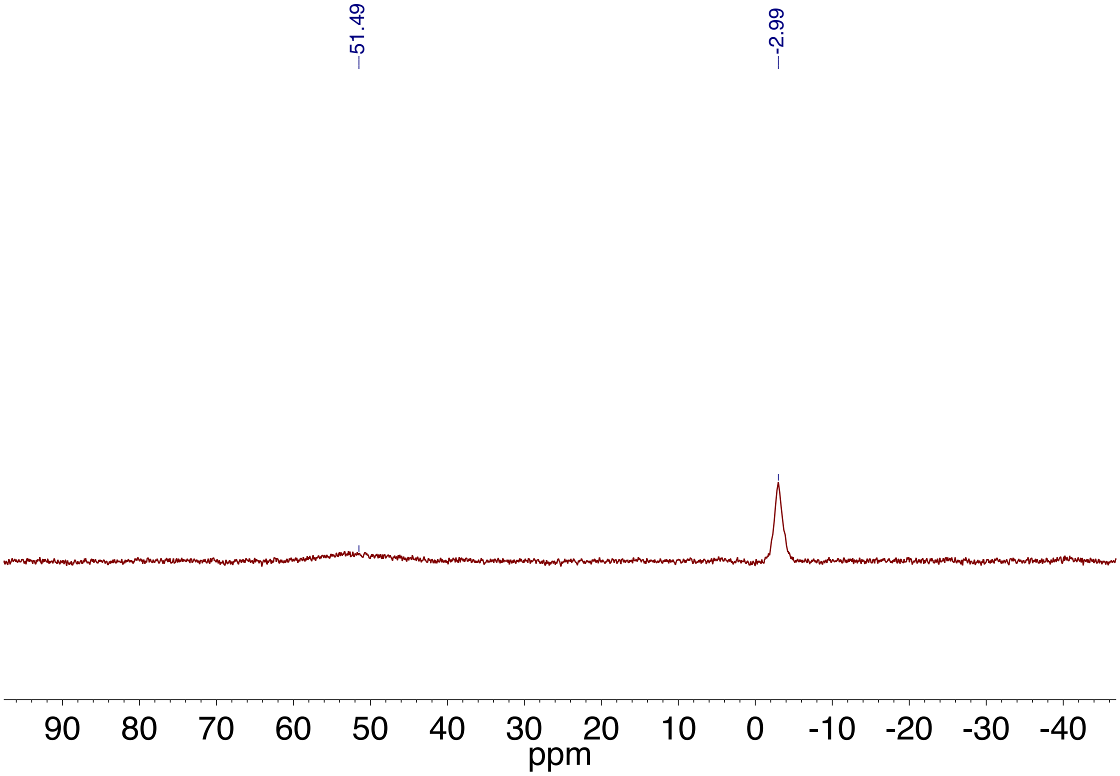

Figure S30. ^{11}B NMR spectrum of [Au(B$_2$P$_2$)](O(Si^{i}Pr$_3$) (**9**) recorded at 160 MHz in C$_6$D$_6$.

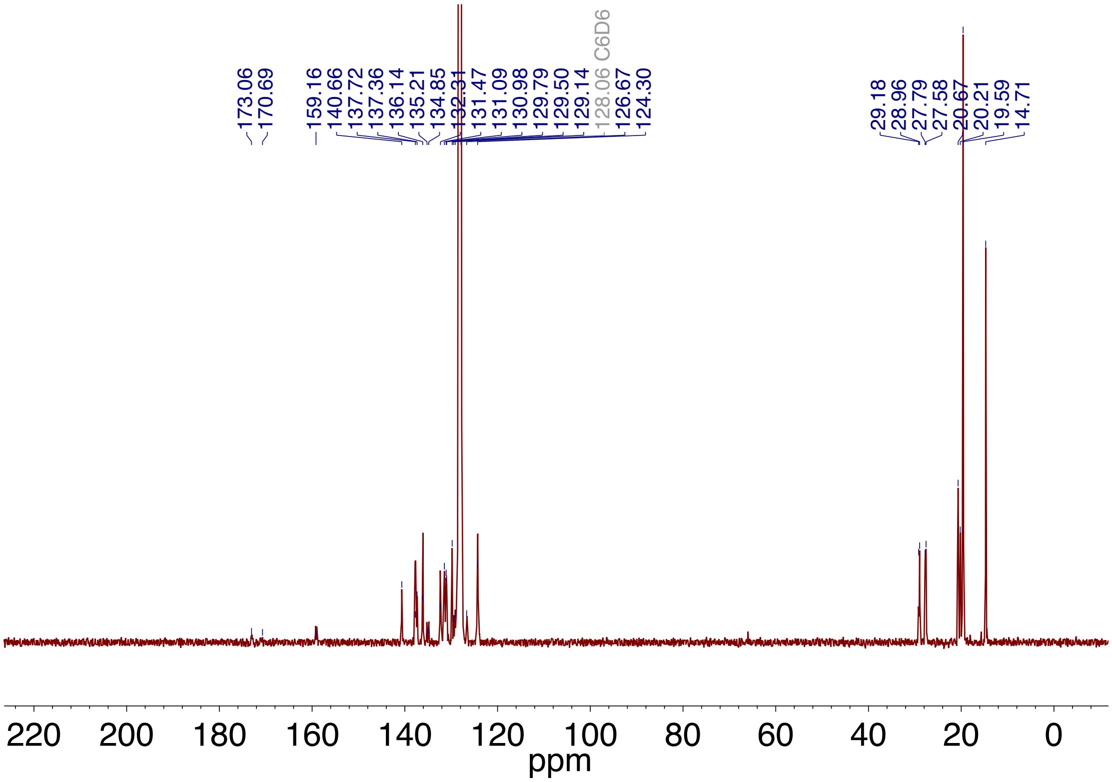

Figure S31. $^{13}C\{^{1}H\}$ NMR spectrum of $[Au(B_2P_2)](O(Si^iPr_3)$ (**9**) recorded at 126 MHz in C_6D_6.

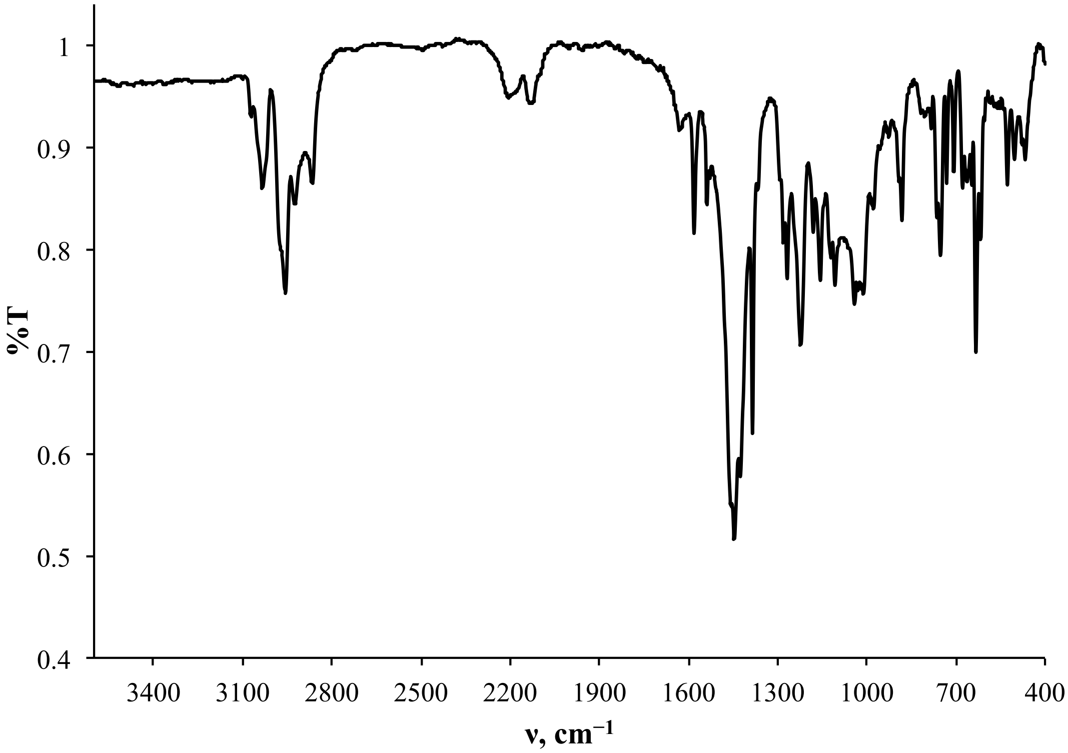

Figure S32. FT-IR spectrum of $[Au(B_2P_2)]H$ (**2**).

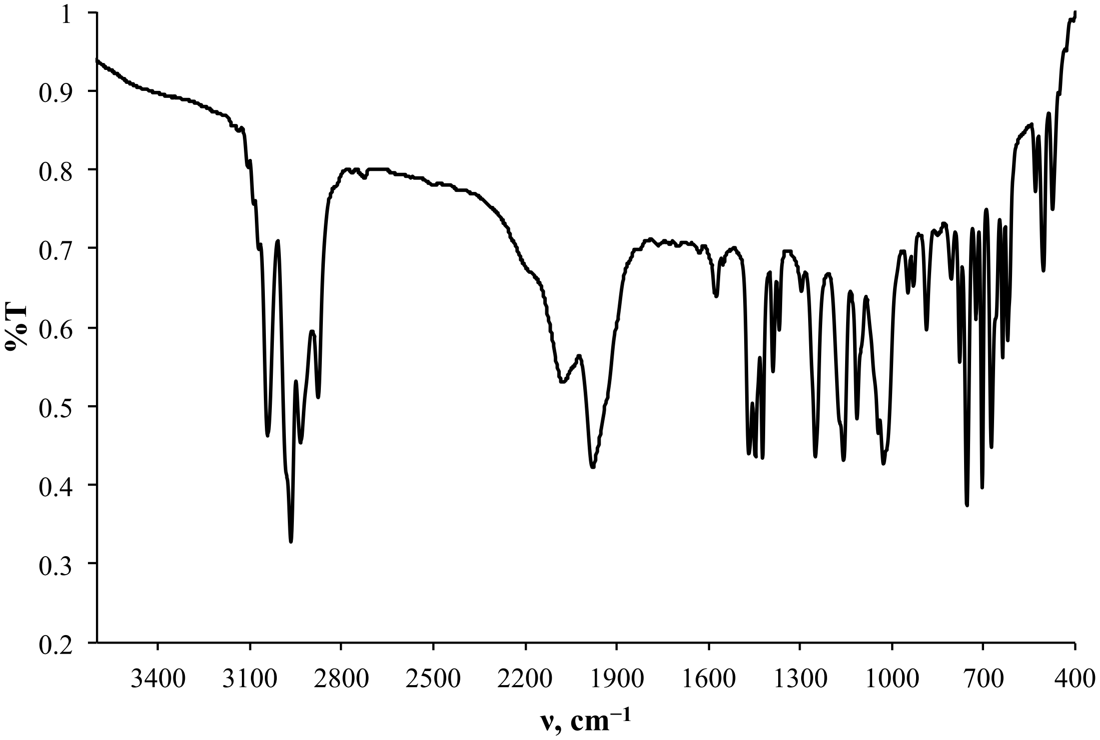

Figure S33. FT-IR spectrum of $[Au(B_2P_2)(H_2)][K(Et_2O)]$ (**6**).

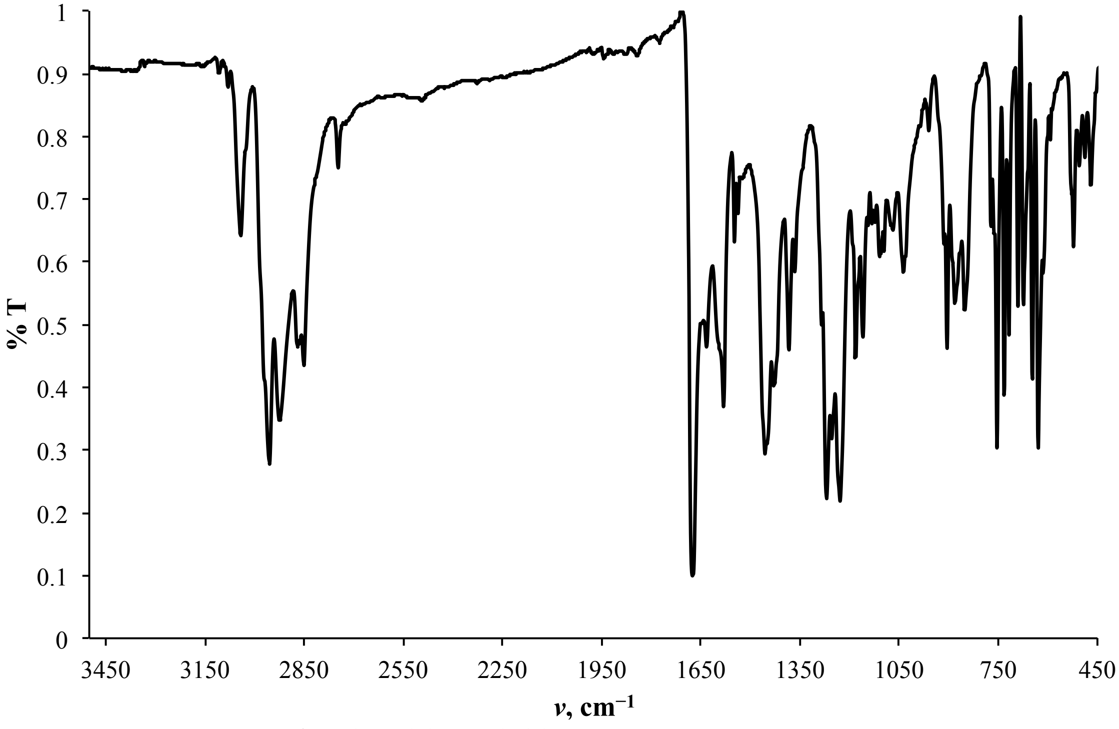

Figure S34. FT-IR spectrum of $Au(B_2P_2)(CO_2H)$ (**5**).

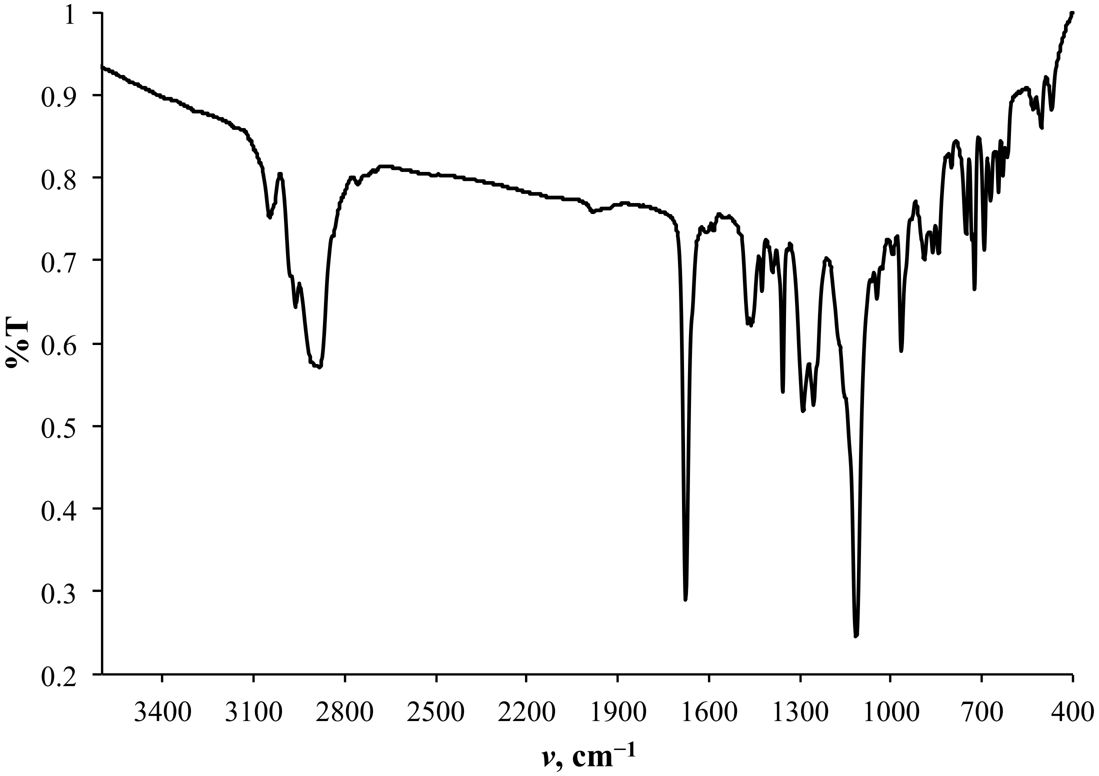

Figure S35. FT-IR spectrum of $[Au(B_2P_2)(CO_2H)_2][K(18\text{-}c\text{-}6)]$ (**7**).

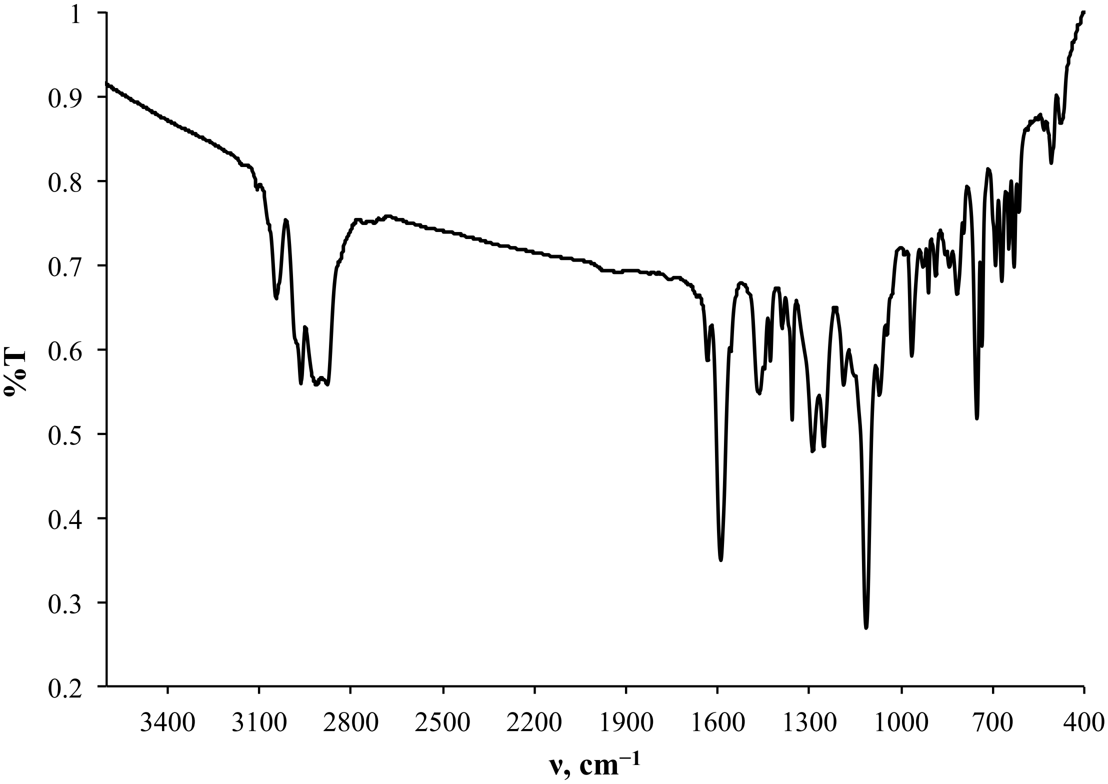

Figure S36. FT-IR spectrum of $[Au(B_2P_2)(CO_3)][K(18c6)]$ (**8**).

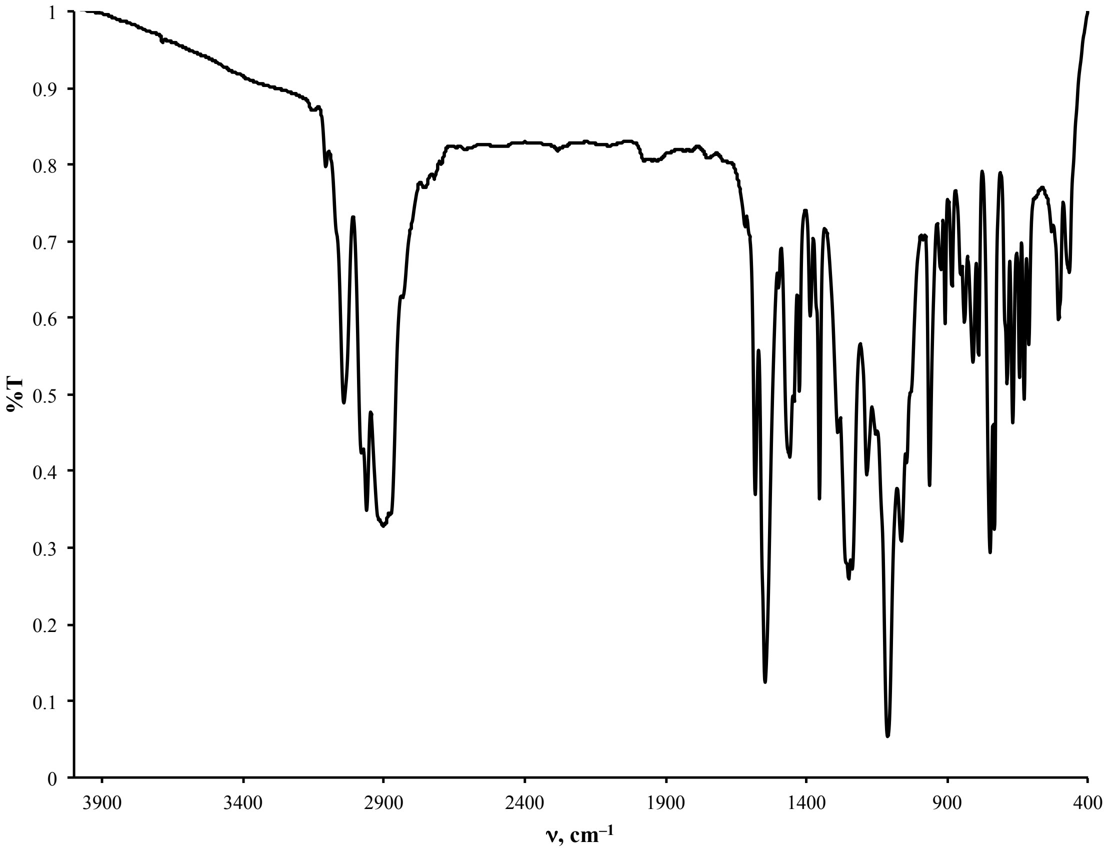

Figure S37. FT-IR spectrum of [Au(B_2P_2)($^{13}CO_3$)][K(18-c-6)] (**8-^{13}C**).

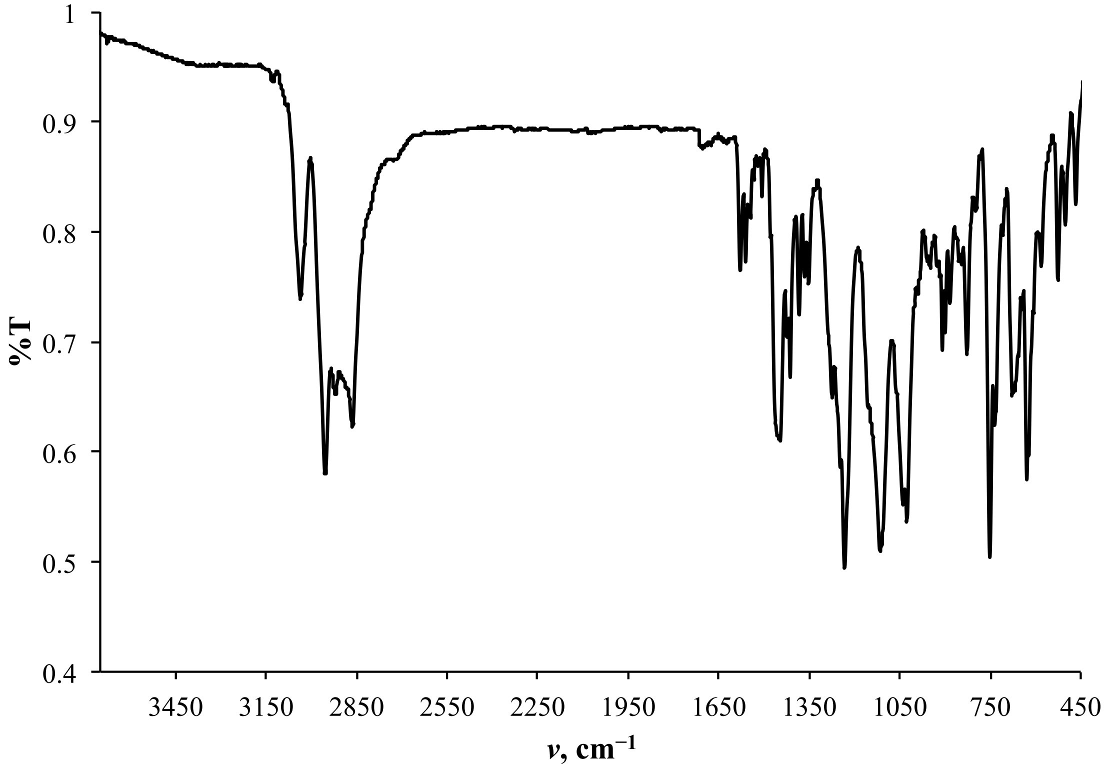

Figure S38. FT-IR spectrum of [Au(B_2P_2)(OSi^{i}Pr$_3$)] (**9**).

X-Ray Crystallography

General Considerations. Single crystals were coated with paratone oil and mounted on cryo-loop glass fibers. X-ray intensity data were collected at 100(2) K on a Bruker APEX2[6] platform-CCD X-ray diffractometer system using fine-focus Mo K_α radiation (λ = 0.71073 Å, 50kV/30mA power). The CCD detector was placed at 5.0600 cm from the crystal. Frames were integrated using the Bruker SAINT software package[7] and using a narrow-frame integration algorithm. Absorption corrections were applied to the raw intensity data using the SADABS program.[8] The Bruker SHELXTL software package[9] was used for phase determination and structure refinement. Atomic coordinates, isotropic and anisotropic displacement parameters of all the non-hydrogen atoms were refined by means of a full matrix least-squares procedure on F^2. The H-atoms were included in the refinement in calculated positions riding on the atoms to which they were attached. Relevant details for individual data collections are reported in Tables S1–S6.

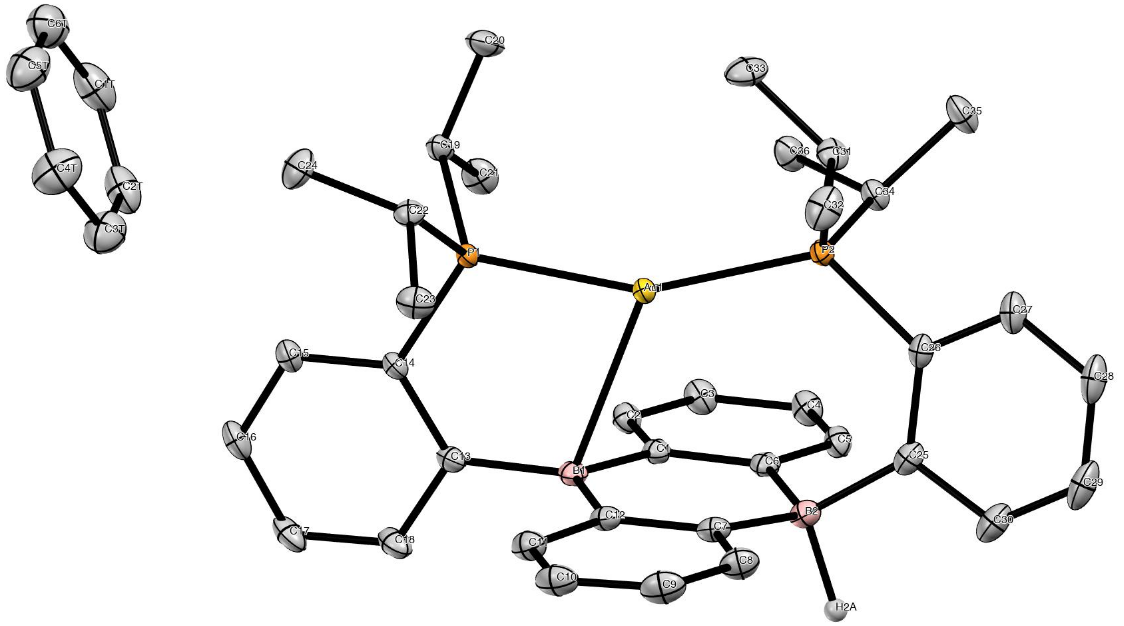

Figure S39. Labelled thermal ellipsoid plot (50%) for Au(B_2P_2)H (**2**).

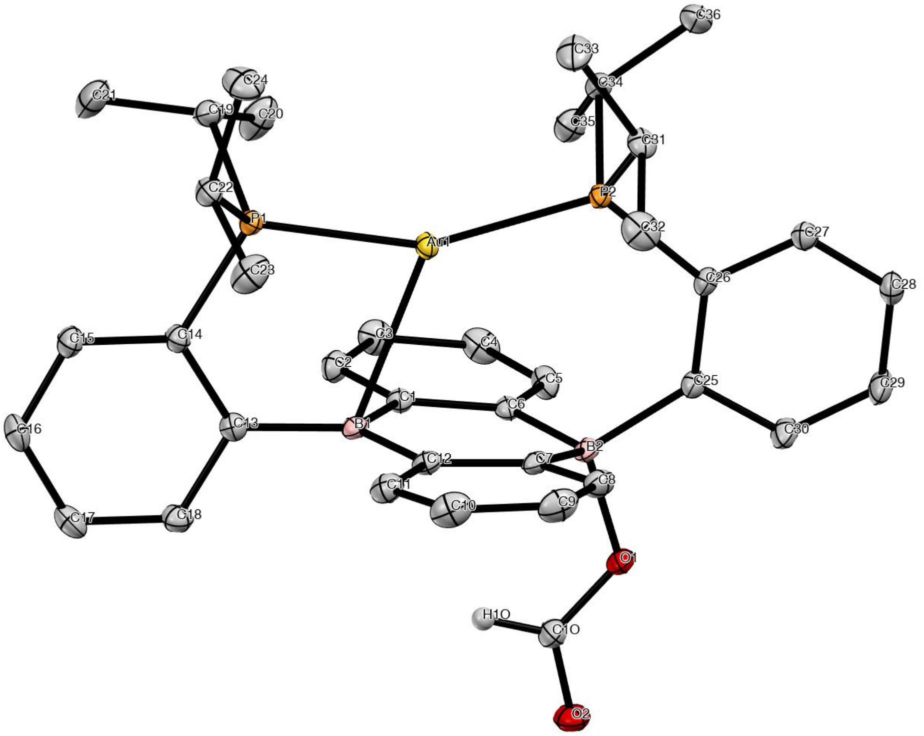

Figure S40. Labelled thermal ellipsoid plot (50%) for Au(B_2P_2)(CO_2H) (**5**).

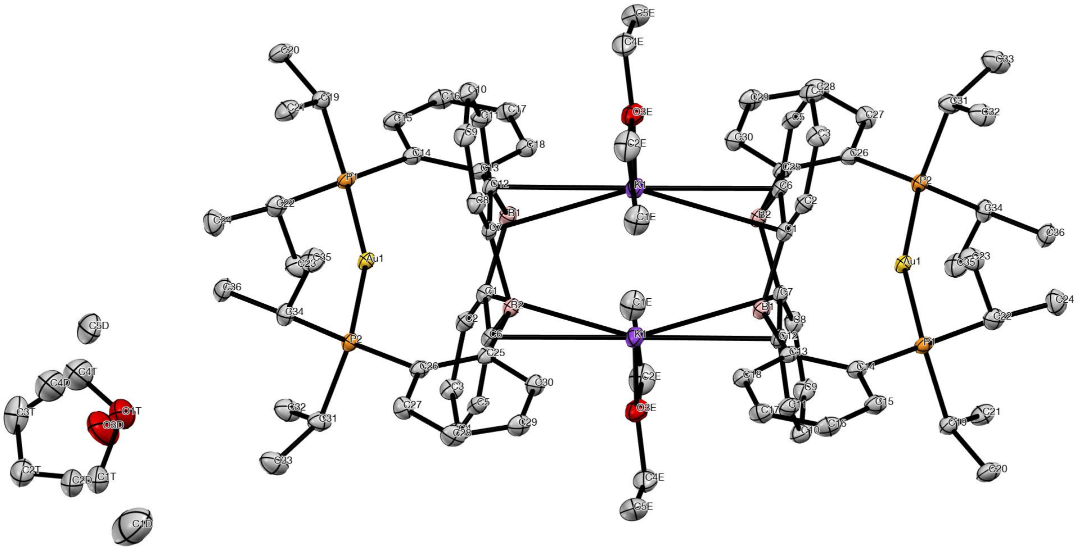

Figure S41. Labelled thermal ellipsoid plot (50%) for $[Au(B_2P_2)H][K(Et_2O)]$ (**6**).

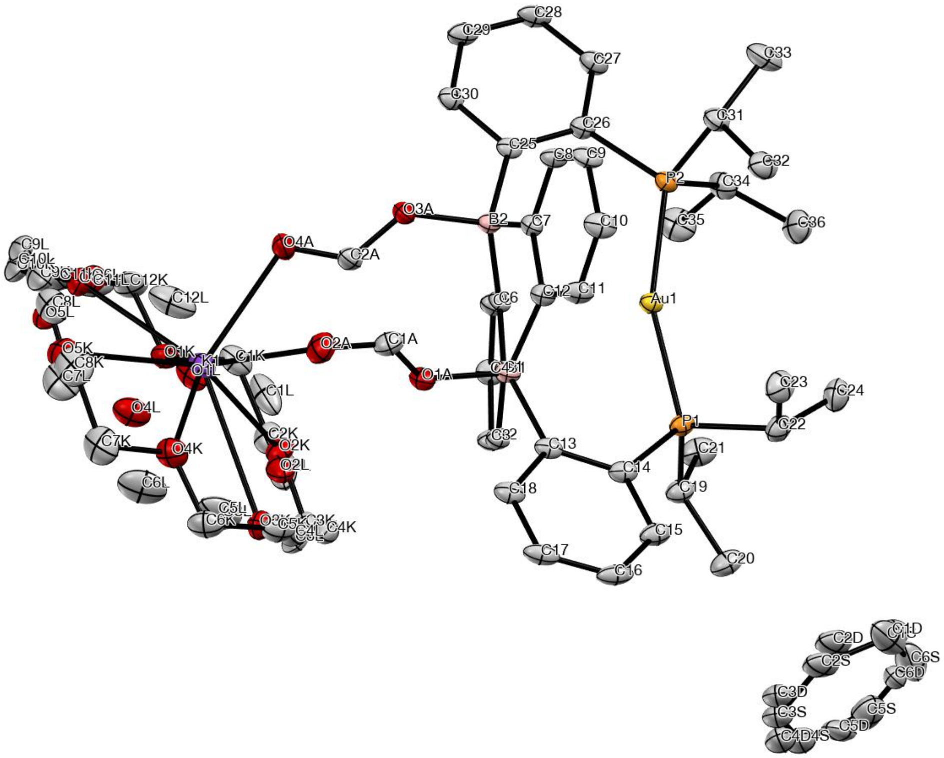

Figure S42. Labelled thermal ellipsoid plot (50%) for $[Au(B_2P_2)(CO_2H)_2][K(18\text{-c-}6)]$ (**7**).

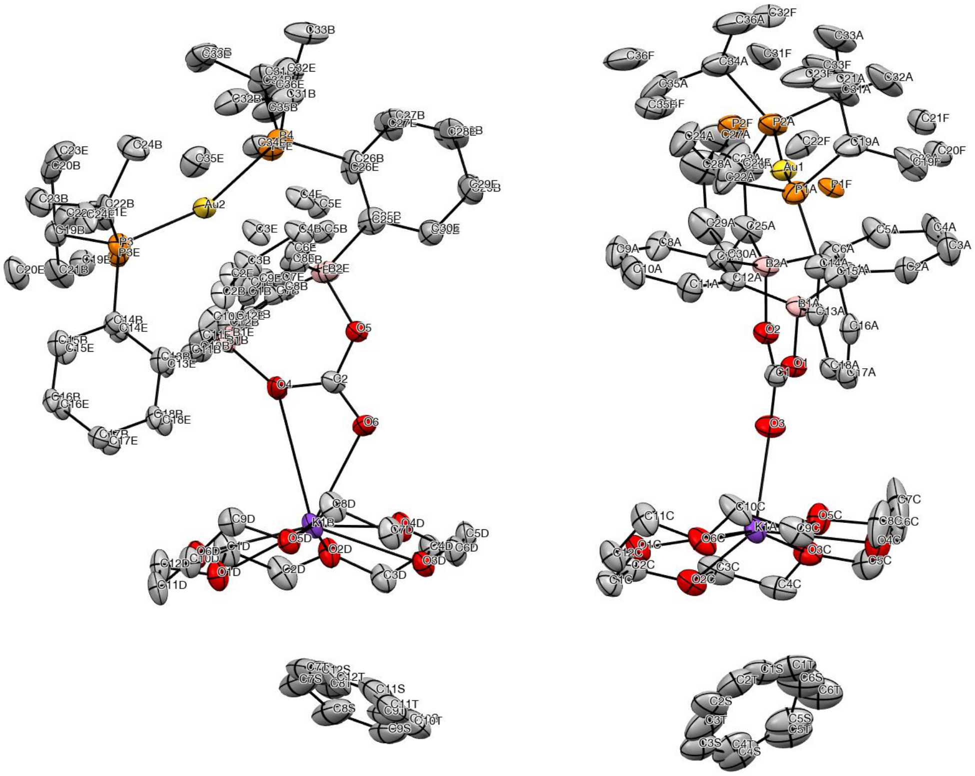

Figure S43. Labelled thermal ellipsoid plot (50%) for $[Au(B_2P_2)(CO_3)][K(18\text{-}c\text{-}6)]$ (**8**).

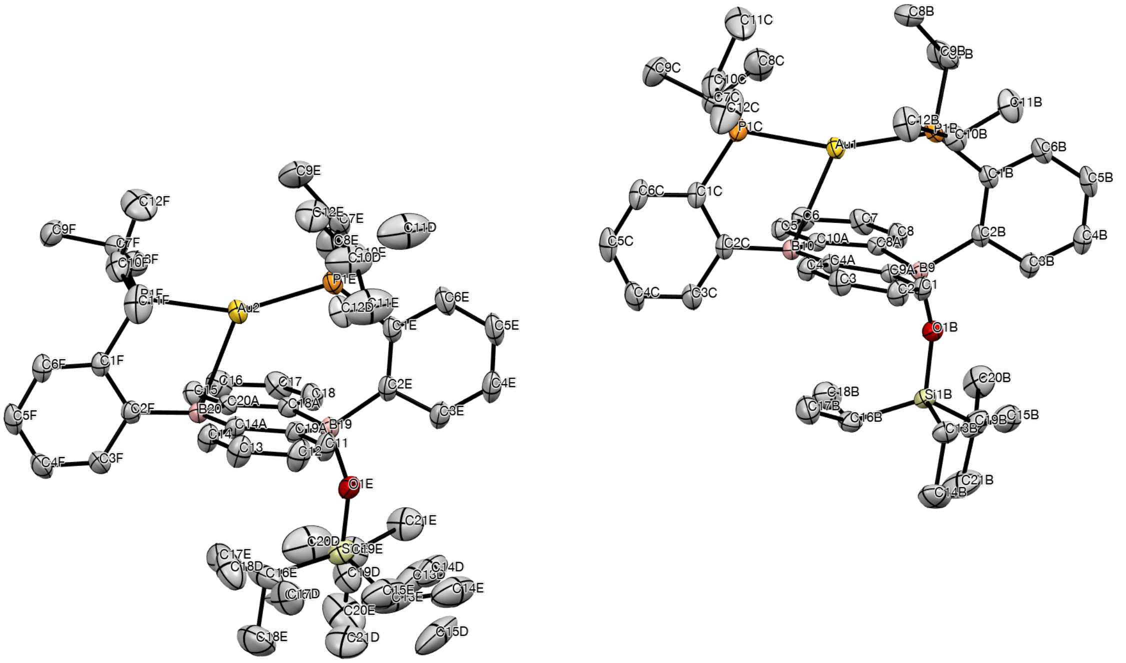

Figure S44. Labelled thermal ellipsoid plot (50%) for $Au(B_2P_2)OSi^iPr_3)$ (**9**).

Table S1. Crystal data and structure refinement for Au(B_2P_2)H (**2**).

Identification code	hh94JT43_0m	
Empirical formula	$C_{42}H_{51}AuB_2P_2$	
Formula weight	836.35 g/mol	
Temperature	100(2) K	
Wavelength	0.71073 Å	
Crystal system	Monoclinic	
Space group	P 21/c	
Unit cell dimensions	a = 13.6605(2) Å	α = 90°.
	b = 18.5231(3) Å	β = 97.9128(5)°.
	c = 14.7583(2) Å	γ = 90°.
Volume	3698.81(10) $Å^3$	
Z	4	
Density (calculated)	1.502 mg/m^3	
Absorption coefficient	4.093 mm^{-1}	
F(000)	1688	
Crystal size	0.508 x 0.221 x 0.162 mm^3	
θ range for data collection	1.775 to 34.336°.	
Index ranges	$-21 \leq h \leq 21$, $-29 \leq k \leq 29$, $-23 \leq l \leq 23$	
Reflections collected	236591	
Independent reflections	15490 [R_{int} = 0.0303]	
Completeness to θ = 25.242°	100.0 %	
Absorption correction	Semi-empirical from equivalents	
Refinement method	Full-matrix least-squares on F^2	
Data / restraints / parameters	15490 / 0 / 435	
Goodness-of-fit on F^2	1.035	
Final R indices [$I > 2\sigma_I$]	R_1 = 0.0161, wR_2 = 0.0373	
R indices (all data)	R_1 = 0.0203, wR_2 = 0.0386	
Largest diff. peak and hole	1.230 and –0.708 e/$Å^3$	

Table S2. Crystal data and structure refinement for **$Au(B_2P_2)(CO_2H)$ (5)**.

Identification code	hh108JT52_0m	
Empirical formula	$C_{37}H_{45}AuB_2O_2P_2$	
Formula weight	802.25 g/mol	
Temperature	100(2) K	
Wavelength	0.71073 Å	
Crystal system	Monoclinic	
Space group	P 21/c	
Unit cell dimensions	a = 10.7350(4) Å	α = 90°.
	b = 19.4697(6) Å	β = 107.5607(5)°.
	c = 16.9388(6) Å	γ = 90°.
Volume	3375.3(2) $Å^3$	
Z	4	
Density (calculated)	1.579 mg/m^3	
Absorption coefficient	4.486 mm^{-1}	
$F(000)$	1608	
Crystal size	0.361 x 0.283 x 0.202 mm^3	
θ range for data collection	1.638 to 30.034°.	
Index ranges	$-15 \leq h \leq 15, -27 \leq k \leq 27, -23 \leq l \leq 23$	
Reflections collected	95114	
Independent reflections	9868 [R_{int} = 0.0260]	
Completeness to θ = 25.242°	100.0 %	
Absorption correction	Semi-empirical from equivalents	
Refinement method	Full-matrix least-squares on F^2	
Data / restraints / parameters	9868 / 0 / 405	
Goodness-of-fit on F^2	1.049	
Final R indices [$I > 2\sigma_I$]	R_1 = 0.0149, wR_2 = 0.0353	
R indices (all data)	R_1 = 0.0176, wR_2 = 0.0362	
Largest diff. peak and hole	0.924 and –0.291 e/$Å^3$	

Table S3. Crystal data and structure refinement for $[\mathrm{Au(B_2P_2)H_2}][\mathrm{K(Et_2O)}]$ (**6**).

Identification code	hh190JT93r_0m	
Empirical formula	$C_{88}H_{128.50}Au_2B_4K_2O_4P_4$	
Formula weight	1889.65 g/mol	
Temperature	100(2) K	
Wavelength	0.71073 Å	
Crystal system	Monoclinic	
Space group	P 21/n	
Unit cell dimensions	a = 17.3226(5) Å	$\alpha = 90°$.
	b = 14.0750(4) Å	$\beta = 108.2727(5)°$.
	c = 18.5251(5) Å	$\gamma = 90°$.
Volume	4289.0(2) $Å^3$	
Z	2	
Density (calculated)	1.463 mg/m^3	
Absorption coefficient	3.637 mm^{-1}	
$F(000)$	1929	
Crystal size	0.321 x 0.193 x 0.102 mm^3	
θ range for data collection	1.853 to 30.508°.	
Index ranges	$-24 \leq h \leq 24$, $-20 \leq k \leq 20$, $-26 \leq l \leq 26$	
Reflections collected	101496	
Independent reflections	13085 [R_{int} = 0.0375]	
Completeness to θ = 25.242°	100.0 %	
Absorption correction	Semi-empirical from equivalents	
Refinement method	Full-matrix least-squares on F^2	
Data / restraints / parameters	13085 / 38 / 521	
Goodness-of-fit on F^2	1.060	
Final R indices [$I > 2\sigma_I$]	$R_1 = 0.0211$, $wR_2 = 0.0398$	
R indices (all data)	$R_1 = 0.0326$, $wR_2 = 0.0429$	
Largest diff. peak and hole	1.030 and –0.977 e/$Å^3$	

Notes: There was half a molecule of $C_{72}H_{92}Au_2B_4K_2P_4.[C_4H_{10}O]_2$, and one $[C_4H_{10}O]/[C_4H_8O]$ disordered solvents (disordered site occupancy ratio was 87%/13%) present in the asymmetric unit of the unit cell. The $C_{72}H_{92}Au_2B_4K_2P_4.[C_4H_{10}O]_2$ molecule was located at the inversion symmetry. The short intermolecular contacts H33A...H1G and C33...C1D are due to the $[C_4H_{10}O]/[C_4H_8O]$ disordered solvents.

Table S4. Crystal data and structure refinement for $[Au(B_2P_2)(CO_2H)_2][K(18\text{-}c\text{-}6)]$ (**7**).

Identification code	hh218JT106_0m	
Empirical formula	$C_{56}H_{76}AuB_2KO_{10}P_2$	
Formula weight	1228.79 g/mol	
Temperature	100(2) K	
Wavelength	0.71073 Å	
Crystal system	Triclinic	
Space group	P –1	
Unit cell dimensions	a = 9.4884(3) Å	α = 82.1272(5)°.
	b = 16.6011(5) Å	β = 83.3368(5)°.
	c = 18.4187(5) Å	γ = 81.8270(5)°.
Volume	2830.91(15) $Å^3$	
Z	2	
Density (calculated)	1.442 mg/m^3	
Absorption coefficient	2.784 mm^{-1}	
F(000)	1260	
Crystal size	0.332 x 0.153 x 0.083 mm^3	
θ range for data collection	1.573 to 28.282°.	
Index ranges	$-12 \leq h \leq 12, -22 \leq k \leq 22, -24 \leq l \leq 24$	
Reflections collected	79048	
Independent reflections	14037 [R_{int} = 0.0329]	
Completeness to θ = 25.242°	100.0 %	
Absorption correction	Semi-empirical from equivalents	
Refinement method	Full-matrix least-squares on F^2	
Data / restraints / parameters	14037 / 96 / 821	
Goodness-of-fit on F^2	1.036	
Final R indices [$I > 2\sigma_I$]	R_1 = 0.0191, wR_2 = 0.0427	
R indices (all data)	R_1 = 0.0221, wR_2 = 0.0439	
Largest diff. peak and hole	0.800 and –0.511 $e/Å^3$	

Notes: There was one molecule of $C_{38}H_{46}B_2O_4P_2Au.KC_{12}H_{24}0_6$ where the crown ether was modeled with disorder (disordered site occupancy ratio was 59%/41%), and one disordered benzene molecule (disordered site occupancy ratio was 69%/31%) present in the asymmetric unit of the unit cell.

Table S5. Crystal data and structure refinement for [Au(B_2P_2)(CO_3)][K(18-c-6)] (**8**).

Identification code	hh233JT117_0m	
Empirical formula	$C_{55}H_{74}AuB_2KO_9P_2$	
Formula weight	1198.76 g/mol	
Temperature	100(2) K	
Wavelength	0.71073 Å	
Crystal system	Triclinic	
Space group	P –1	
Unit cell dimensions	a = 17.085(3) Å	α = 91.133(2)°.
	b = 17.761(3) Å	β = 91.253(2)°.
	c = 18.264(3) Å	γ = 90.383(2)°.
Volume	5539.7(15) $Å^3$	
Z	4	
Density (calculated)	1.437 mg/m^3	
Absorption coefficient	2.842 mm^{-1}	
F(000)	2456	
Crystal size	0.564 x 0.122 x 0.040 mm^3	
θ range for data collection	1.584 to 25.681°.	
Index ranges	$-20 \leq h \leq 20$, $-21 \leq k \leq 21$, $-22 \leq l \leq 22$	
Reflections collected	65770	
Independent reflections	20977 [R_{int} = 0.0623]	
Completeness to θ = 25.242°	99.8 %	
Absorption correction	Semi-empirical from equivalents	
Refinement method	Full-matrix least-squares on F^2	
Data / restraints / parameters	20977 / 18 / 1501	
Goodness-of-fit on F^2	1.036	
Final R indices [$I > 2\sigma_I$]	R_1 = 0.0464, wR_2 = 0.0972	
R indices (all data)	R_1 = 0.0677, wR_2 = 0.1063	
Largest diff. peak and hole	2.966 and –1.520 e/$Å^3$	

Notes: There were two disordered molecules of $C_{55}H_{74}B_2O_9P_2KAu$ present in the asymmetric unit of the unit cell. The two disordered benzene were coordinated to the two K-atoms (disordered site occupancy ratios were 56%/44% and 67%/33%). The two disordered ligands were coordinated to the two Au-atoms (disordered site occupancy ratios were 76%/24% and 51%/49%).

Table S6. Crystal data and structure refinement for Au(B_2P_2)(OSi^{i}Pr$_3$) (**9**).

Identification code	hh241JT120_0m	
Empirical formula	$C_{45}H_{65}AuB_2OP_2Si$	
Formula weight	930.58 g/mol	
Temperature	180(2) K	
Wavelength	0.71073 Å	
Crystal system	Monoclinic	
Space group	$P2_1/c$	
Unit cell dimensions	a = 20.6988(5) Å	α = 90°.
	b = 22.0547(5) Å	β = 92.3184(5)°.
	c = 19.2806(5) Å	γ = 90°.
Volume	8794.5(4) $Å^3$	
Z	8	
Density (calculated)	1.406 mg/m^3	
Absorption coefficient	3.478 mm^{-1}	
F(000)	3808	
Crystal color	light yellow	
Crystal size	0.406 x 0.278 x 0.182 mm^3	
θ range for data collection	1.690 to 29.575°	
Index ranges	$-28 \leq h \leq 28, -30 \leq k \leq 30, -26 \leq l \leq 26$	
Reflections collected	198681	
Independent reflections	24666 [R_{int} = 0.0280]	
Completeness to θ = 25.242°	100.0 %	
Absorption correction	Semi-empirical from equivalents	
Refinement method	Full-matrix least-squares on F^2	
Data / restraints / parameters	24666 / 381 / 1065	
Goodness-of-fit on F^2	1.023	
Final R indices [$I > 2\sigma_I$]	R_1 = 0.0222, wR_2 = 0.0498	
R indices (all data, 0.72 Å)	R_1 = 0.0286, wR_2 = 0.0519	
Largest diff. peak and hole	1.201 and –1.023 e/$Å^3$	

References

[1] J. W. Taylor, A. McSkimming, C. F. Guzman, W. H. Harman, *J. Am. Chem. Soc.* 2017, **139**, 11032.
[2] Z. Yang, L. N. He, C. X. Miao, S. Chanfreau, *Adv. Synth. Catal.* 2010, **352**, 2233.
[3] T. A. Scott, B. A. Ooro, D. J. Collins, M. Shatruk, A. Yakovenko, K. R. Dunbar, H.-C. Zhou, *Chem. Commun.* 2009, **1**, 65.
[4] J. J. Led, H. Gesmar, *Chem. Rev.* 1991, **91**, 1413.
[5] H. E. Gottlieb, V. Kotlyar, A. Nudelman, *J. Org. Chem.* 1997, **62**, 7512.
[6] APEX 2, version 2014.1-1, Bruker (2014), Bruker AXS Inc., Madison, Wisconsin, USA.
[7] SAINT, version V8.34A, Bruker (2012), Bruker AXS Inc., Madison, Wisconsin, USA.
[8] SADABS, version 2012/1, Bruker (2012), Bruker AXS Inc., Madison, Wisconsin, USA.
[9] SHELXTL, version 2013/4, Bruker (2013), Bruker AXS Inc., Madison, Wisconsin, USA.